

A Third-Order Accurate Direct Eulerian GRP Scheme for One-Dimensional Relativistic Hydrodynamics

Kailiang Wu, Zhicheng Yang and Huazhong Tang*

HEDPS, CAPT & LMAM, School of Mathematical Sciences, Peking University, Beijing 100871, P.R. China.

Received 10 October 2013; Accepted (in revised version) 10 March 2014

Available online 7 April 2014

Abstract. A third-order accurate direct Eulerian generalised Riemann problem (GRP) scheme is derived for the one-dimensional special relativistic hydrodynamical equations. In our GRP scheme, the higher-order WENO initial reconstruction is employed, and the local GRPs in the Eulerian formulation are directly and analytically resolved to third-order accuracy via the Riemann invariants and Rankine-Hugoniot jump conditions, to get the approximate states in numerical fluxes. Unlike a previous second-order accurate GRP scheme, for the non-sonic case the limiting values of the second-order time derivatives of the fluid variables at the singular point are also needed for the calculation of the approximate states; while for the sonic case, special attention is paid because the calculation of the second-order time derivatives at the sonic point is difficult. Several numerical examples are given to demonstrate the accuracy and effectiveness of our GRP scheme.

AMS subject classifications: 65M06, 76M12, 76Y05

Key words: Godunov-type scheme, WENO, generalised Riemann problem, Riemann invariant, Rankine-Hugoniot jump condition, relativistic hydrodynamics.

1. Introduction

If the fluid velocity is locally close to light speed in a vacuum or the internal energy density is locally comparable (or larger) than the fluid rest-mass density, a relativistic description of the fluid dynamics should be adopted. Moreover, the Einstein field theory of gravity is appropriate whenever the matter is influenced by large gravitational potentials. Relativistic flows arise in numerous astrophysical phenomena, from stellar to galactic scales — e.g. active galactic nuclei, super-luminal jets, core collapse super-novae, pulsars, coalescing neutron stars, black holes, micro-quasars, X-ray binaries, and gamma-ray bursts.

*Corresponding author. *Email addresses:* wukl@pku.edu.cn (K. L. Wu), yangzhicheng@foxmail.com (Z. C. Yang), hztang@math.pku.edu.cn (H. Z. Tang)

Theoretical relativistic flow dynamics involves solving highly nonlinear equations, where an analytic treatment is extremely difficult so that numerical studies are important. The earliest numerical study can be traced to Ref. [16], where the general relativistic hydrodynamic (RHD) equations in Eulerian form are solved by an explicit finite difference method using an artificial viscosity. Subsequently, other relevant finite difference methods were systematically introduced [17]. Various modern shock-capturing methods based on exact or approximate Riemann solvers have since been developed for the RHD equations — cf. the review articles [5, 13], and more recent overviews of numerical methods for the RHD equations [18, 24]. Second-order accurate direct Eulerian generalised Riemann problem (GRP) schemes have recently been proposed for both 1D and 2D relativistic hydrodynamics [21, 22]. An analytic extension of the Godunov method, the GRP scheme was originally devised for non-relativistic compressible fluid dynamics [1], by utilising a piecewise linear function to approximate the initial data and then analytically resolving a local GRP at each interface to yield numerical fluxes — cf. the comprehensive description in Ref. [2] and references therein.

The original GRP scheme has two versions, Lagrangian and the Eulerian. The Eulerian form is always derived using the Lagrangian framework, which has the advantage that the contact discontinuity in each local wave pattern is always fixed with speed zero and the nonlinear waves are located on either side. However, the passage from the Lagrangian framework to the Eulerian form is sometimes quite delicate, particularly for the sonic case and multi-dimensional applications. To avoid the difficulty, second-order accurate direct Eulerian GRP schemes were respectively developed for the shallow water equations [8], the Euler equations [4], the governing equations for the gas-liquid two-phase flow in HTHP transient wells [20], and a more general weakly coupled system [3] by directly and analytically resolving the local GRPs in the Eulerian formulation via Riemann invariants and the Rankine-Hugoniot jump conditions. The GRP scheme has been compared with the gas-kinetic scheme for inviscid compressible flow simulations [9]. In Ref. [6], the adaptive direct Eulerian GRP scheme was further developed with improved resolution as well as accuracy by combining the moving mesh method [15]; and the accuracy and performance of the adaptive GRP scheme was further studied in simulating 2D complex wave configurations formulated via 2D Riemann problems from compressible Euler equations [7].

The aim of this article is to derive a third-order accurate direct Eulerian GRP scheme for the 1D special RHD equations analytically, extending the recent second-order accurate direct Eulerian GRP scheme for the RHD equations [21, 22] and the third-order accurate direct Eulerian GRP scheme for 1D and 2D non-relativistic Euler equations [19]. In passing, we note that a unified approach for solving the GRP with higher-order accuracy has been provided for general 1D hyperbolic balance laws [14]. Section 2 introduces the 1D special RHD equations and corresponding Riemann invariants as well as their basic properties. The third-order accurate GRP scheme for the 1D RHD equations is derived analytically in Section 3. The scheme is first outlined in Section 3.1, and the local GRPs are resolved in Section 3.2 — with the rarefaction and shock waves respectively discussed in Subsections 3.2.1 and 3.2.2, the approximate states in numerical fluxes separately for both non-sonic and sonic cases in Subsection 3.2.3, and the acoustic case in Subsection 3.2.3.

Several numerical experiments discussed in Section 4 demonstrate the performance and accuracy of our proposed GRP scheme, and our conclusions are summarised in Section 5.

2. Preliminaries and Notation

This section introduces the 1D special RHD equations and corresponding Riemann invariants, and their basic properties.

2.1. Governing equations

The covariant form of the four-dimensional space-time relativistic hydrodynamical (RHD) equations appear widely in the literature [17] and the RHD equations may be written as a first-order hyperbolic system that can be advanced forward in time by using the modern shock-capturing methods in some fixed or rest reference frame, often called the laboratory frame (the reference frame of the observer). The 1D RHD equations can thus be cast into the conservative form

$$\begin{aligned} U_t + F(U)_x &= 0, \\ U &= (D, m, E)^T, \quad F = (Du, mu + p, m)^T, \end{aligned} \quad (2.1)$$

where $D = \gamma\rho$, $m = Dh\gamma u$ and $E = Dh\gamma - p$ denote the mass, x -momentum and energy densities relative to the laboratory frame respectively, while ρ and p , u and $\gamma = 1/\sqrt{1-u^2}$ are the rest-mass density, the kinetic pressure, the fluid velocity and the Lorentz factor respectively. Here h is the specific enthalpy defined by

$$h = 1 + e + \frac{p}{\rho},$$

where e denotes the specific internal energy. An equation of state, a relation between thermodynamical variables such as $p = p(\rho, e)$, is needed to close the system (2.1). For ideal gases, the equation of state has the form

$$p = (\Gamma - 1)\rho e, \quad (2.2)$$

where Γ is the adiabatic index.

In a smooth region, the system (2.1) may be recast into the equivalent nonconservative form

$$\begin{cases} \frac{\mathcal{D}S}{\mathcal{D}t} = 0, \\ \frac{\mathcal{D}u}{\mathcal{D}t} = \frac{uc_s^2}{\gamma^2(1-u^2c_s^2)} \frac{\partial u}{\partial x} - \frac{1}{\rho h \gamma^4(1-u^2c_s^2)} \frac{\partial p}{\partial x}, \\ \frac{\mathcal{D}p}{\mathcal{D}t} = \frac{uc_s^2}{\gamma^2(1-u^2c_s^2)} \frac{\partial p}{\partial x} - \frac{\rho h c_s^2}{1-u^2c_s^2} \frac{\partial u}{\partial x}, \end{cases} \quad (2.3)$$

$$\begin{cases} \frac{\mathcal{D}\rho}{\mathcal{D}t} = \frac{1}{hc_s^2} \frac{\mathcal{D}p}{\mathcal{D}t}, \\ \frac{\partial u}{\partial x} = -\gamma^2 \left(u \frac{\mathcal{D}u}{\mathcal{D}t} + \frac{1}{\rho h \gamma^2 c_s^2} \frac{\mathcal{D}p}{\mathcal{D}t} \right), \\ \frac{\partial p}{\partial x} = -\gamma^2 \left(\rho h \gamma^2 \frac{\mathcal{D}u}{\mathcal{D}t} + \frac{\mathcal{D}p}{\mathcal{D}t} \right), \end{cases} \quad (2.4)$$

and

$$V_t + A(V)V_x = 0, \quad A(V) = \begin{pmatrix} u & \frac{\rho}{1-u^2c_s^2} & \frac{u(u^2-1)}{h(1-u^2c_s^2)} \\ 0 & \frac{u(1-c_s^2)}{1-u^2c_s^2} & \frac{1}{\rho h \gamma^4 (1-u^2c_s^2)} \\ 0 & \frac{\rho h c_s^2}{1-u^2c_s^2} & \frac{u(1-c_s^2)}{1-u^2c_s^2} \end{pmatrix}, \quad (2.5)$$

where $\mathbf{V} = (\rho, u, p)^T$, $\mathcal{D}/\mathcal{D}t := \partial_t + u\partial_x$ denotes the total derivative operator along the trajectory of the fluid particle defined by $dx/dt = u$, c_s is the sound speed defined by

$$c_s^2 = \frac{1}{h} \frac{\partial p(\rho, S)}{\partial \rho} = \frac{1}{h} \left(\frac{\partial p(\rho, e)}{\partial \rho} + \frac{p}{\rho^2} \frac{\partial p(\rho, e)}{\partial e} \right), \quad (2.6)$$

and S denotes the specific entropy related to the other thermodynamical variables through the thermodynamic relation

$$T dS = de - \frac{p}{\rho^2} d\rho \quad (2.7)$$

where T is the temperature.

The RHD equations (2.1) are identical in formal structure to the 1D non-relativistic Euler equations, and may be reduced to those equations when the fluid velocity is small ($|u| \ll 1$) and the velocity of the internal (microscopic) motion of the fluid particles is small. However, relations between the laboratory quantities (D , m , and E) and the quantities in the local rest frame (e , ρ , and u) introduce a strong coupling between the equations and pose additional numerical difficulties than in the non-relativistic case. For example, the physical constraints $E \geq D$ and $|u| < 1$ have to be fulfilled.

2.2. Riemann invariants

Three eigenvalues of the Jacobian matrix $\partial \mathbf{F}(U)/\partial U$ of the system (2.1) with the equation of state $p = p(\rho, e)$ are

$$\lambda_- = \frac{u - c_s}{1 - uc_s}, \quad \lambda_0 = u, \quad \lambda_+ = \frac{u + c_s}{1 + uc_s},$$

where the first and third characteristic fields are genuinely nonlinear while the second is linearly degenerate. Associated with those genuinely nonlinear characteristic fields λ_{\pm} , the (generalised) Riemann invariants are

$$\psi_{\pm} = \frac{1}{2} \ln \left(\frac{1+u}{1-u} \right) \mp \int^{\rho} \frac{c_s(\omega, S)}{\omega} d\omega, \quad S. \quad (2.8)$$

On regarding all the thermodynamic variables as functions of ρ and S (or p and S), the total differentials of the Riemann invariants ψ_{\pm} have the forms

$$\begin{aligned} d\psi_{\pm} &= \frac{du}{1-u^2} \mp \left(\frac{c_s}{\rho} d\rho + \left(\int^{\rho} \frac{1}{\omega} \frac{\partial c_s(\omega, S)}{\partial S} d\omega \right) dS \right) \\ &= \frac{du}{1-u^2} \mp \left(\frac{1}{\rho h c_s} dp + K(\rho, S) dS \right), \end{aligned} \quad (2.9)$$

where

$$K(\rho, S) = -\frac{1}{\rho h c_s} \frac{\partial p}{\partial S} + \int^{\rho} \frac{1}{\omega} \frac{\partial c_s(\omega, S)}{\partial S} d\omega. \quad (2.10)$$

The total differential forms $d\psi_{\pm}$ in (2.9) reduce to

$$d\psi_{\pm} = \mp K(\rho, S) dS = \mp (\lambda_{\mp} - \lambda_0) K(\rho, S) \frac{\partial S}{\partial x} dt \quad (2.11)$$

along the characteristic curve $dx/dt = \lambda_{\mp}$, thanks to the relations

$$\frac{du}{1-u^2} \pm \frac{dp}{\rho h c_s} = 0, \quad dS = (\lambda_{\pm} - \lambda_0) \frac{\partial S}{\partial x} dt$$

along the characteristic $dx/dt = \lambda_{\pm}$, where the second relation is obtained from the first equation in (2.3).

These Riemann invariants associated with the genuinely nonlinear characteristic fields λ_{\pm} and their total differentials (2.11) play a pivotal role in resolving the centred rarefaction waves in the derivation of the direct Eulerian GRP scheme.

Remark 2.1. For the ideal gas law (2.2), the entropy may be simply written as

$$S := p\rho^{-\Gamma}.$$

In this case, the specific internal energy e and the sound speed c_s may be expressed explicitly as

$$e = \frac{p}{(\Gamma-1)\rho}, \quad c_s^2 = \frac{\Gamma p}{\rho h},$$

and the integral $\int^{\rho} c_s/\omega d\omega$ in the forms (2.8) can be calculated analytically as

$$\int^{\rho} \frac{c_s}{\omega} d\omega = (\Gamma-1)^{-1/2} \ln \left(\frac{(\Gamma-1)^{1/2} + c_s}{(\Gamma-1)^{1/2} - c_s} \right), \quad (2.12)$$

so that

$$K(\rho, S) = \frac{\partial}{\partial S} \int^{\rho} \frac{c_s}{\omega} d\omega - \frac{1}{\rho h c_s} \frac{\partial p}{\partial S} = \frac{1}{\Gamma-1} \frac{1}{\rho h c_s} \frac{\partial p}{\partial S} = \frac{c_s}{(\Gamma-1)\Gamma S}. \quad (2.13)$$

3. Numerical Method

The third-order accurate direct Eulerian GRP scheme for the RHD equations (2.1) is now obtained analytically. For convenience, the spatial domain Ω and time interval $[0, T]$ are respectively divided into the uniform mesh $\{x_j = j\Delta x \in \Omega \mid j \in \mathbb{Z}\}$ and $\{t_n \mid t_0 = 0, t_{n+1} = t_n + \Delta t_n, n \geq 0\}$, where Δx is the spatial step size and the time step size Δt_n is constrained by the stability requirement

$$\Delta t_n = \frac{C_{\text{cfl}} \Delta x}{\max_j \left\{ \left| \lambda_{\pm}(\bar{\mathbf{V}}_{j+\frac{1}{2}}^n) \right| \right\}},$$

in which C_{cfl} denotes the Courant-Friedrichs-Lewy number and $\bar{\mathbf{V}}_{j+\frac{1}{2}}^n$ an approximation of the cell average value of the primitive variable vector $\mathbf{V}(x, t_n)$ over the cell $I_{j+\frac{1}{2}} := (x_j, x_{j+1})$, calculated from the known conservative vector $\bar{\mathbf{U}}_{j+\frac{1}{2}}^n$ by iteratively solving a nonlinear equation — cf. Refs. [21, 22] for a detailed procedure.

3.1. Outline of the third-order accurate GRP scheme

Taking advantage of the cell-average values $\{\bar{\mathbf{V}}_{j+\frac{1}{2}}^n\}$ and any essentially non-oscillatory technique (e.g. the WENO reconstruction mentioned in Remark 3.1), the “initial” function $\mathbf{V}(x, t_n)$ is reconstructed via discontinuous piecewise quadratic polynomial functions

$$\mathbf{V}_h^n(x) = \mathbf{V}_{j+\frac{1}{2}}^{n,(0)} + \mathbf{V}_{j+\frac{1}{2}}^{n,(1)}(x - x_{j+\frac{1}{2}}) + \frac{1}{2} \mathbf{V}_{j+\frac{1}{2}}^{n,(2)}(x - x_{j+\frac{1}{2}})^2 =: \mathbf{V}_{j+\frac{1}{2}}^n(x), \quad x \in I_{j+\frac{1}{2}}. \quad (3.1)$$

The conservative vector \mathbf{U} in (2.1) at time t_{n+1} is approximately evolved by a third-order accurate Godunov-type scheme

$$\bar{\mathbf{U}}_{j+\frac{1}{2}}^{n+1} = \bar{\mathbf{U}}_{j+\frac{1}{2}}^n - \frac{\Delta t_n}{\Delta x} (\hat{\mathbf{F}}_{j+1} - \hat{\mathbf{F}}_j), \quad (3.2)$$

with the numerical flux

$$\hat{\mathbf{F}}_j = \frac{1}{6} \left(\mathbf{F}(\mathbf{U}_j^{n+1,-}) + 4\mathbf{F}(\mathbf{U}_j^{n+1/2}) + \mathbf{F}(\mathbf{U}_j^{\text{RP},n}) \right), \quad (3.3)$$

where $\mathbf{U}_j^{n+1,-} := \mathbf{U}(\mathbf{V}_j^{n+1,-})$ and $\mathbf{U}_j^{n+1/2} := \mathbf{U}(\mathbf{V}_j^{n+1/2})$, with $\mathbf{U}_j^{\text{RP},n}$ the value at $x = x_j$ of the solution to the Riemann problem (RP) for (2.1) and the initial data

$$\mathbf{U}(x, t_n) = \begin{cases} \mathbf{U}_{j,L}^n := \mathbf{U}(\mathbf{V}_h^n(x_j - 0)), & x < x_j, \\ \mathbf{U}_{j,R}^n := \mathbf{U}(\mathbf{V}_h^n(x_j + 0)), & x > x_j, \end{cases}$$

with $\mathbf{V}_j^{n+1/2}$ and $\mathbf{V}_j^{n+1,-}$ calculated case by case. When the transonic rarefaction wave does not appear in the local GRP, we have

$$\begin{cases} \mathbf{V}_j^{n+1/2} = \mathbf{V}_j^{\text{RP},n} + \frac{\Delta t_n}{2} (\mathbf{V}_t)_j^{\text{GRP},n} + \frac{\Delta t_n^2}{8} (\mathbf{V}_{tt})_j^{\text{GRP},n}, \\ \mathbf{V}_j^{n+1,-} = \mathbf{V}_j^{\text{RP},n} + \Delta t_n (\mathbf{V}_t)_j^{\text{GRP},n} + \frac{\Delta t_n^2}{2} (\mathbf{V}_{tt})_j^{\text{GRP},n}, \end{cases} \quad (3.4)$$

where $(\mathbf{V}_t)_j^{\text{GRP},n}$ and $(\mathbf{V}_{tt})_j^{\text{GRP},n}$ are accurately derived by analytically resolving the local GRP for (2.1) with the initial data

$$U(x, t_n) = \begin{cases} U(\mathbf{V}_{j-1/2}^n(x)), & x < x_j, \\ U(\mathbf{V}_{j+1/2}^n(x)), & x > x_j. \end{cases} \quad (3.5)$$

Since the derivations of $\mathbf{U}_j^{\text{RP},n}$ and $(\mathbf{V}_t)_j^{\text{GRP},n}$ are respectively similar to those in [11] and [21], the calculation of $(\mathbf{V}_{tt})_j^{\text{GRP},n}$ given in Section 3.2 below becomes one of the key elements in the current GRP scheme. For the sonic case, because $(\mathbf{V}_{tt})_j^{\text{GRP},n}$ is difficult to resolve at the sonic point, a different calculation of the approximate states $\mathbf{V}_j^{n+1/2}$ and $\mathbf{V}_j^{n+1,-}$ in Eq. (3.3) will be introduced in Section 3.2.3.

Remark 3.1. The polynomial in Eq. (3.1) is obtained through the WENO reconstruction for the characteristic variables $\mathbf{W}(x)$ of (2.5). Concretely, the coefficients $\mathbf{V}_{j+\frac{1}{2}}^{n,(\ell)}$, $\ell = 0, 1, 2$ are calculated as follows [10]:

$$\mathbf{V}_{j+\frac{1}{2}}^{n,(0)} = \frac{3}{2}\bar{\mathbf{V}}_{j+\frac{1}{2}}^n - \frac{1}{2}\mathbf{V}_{j+\frac{1}{2}}^{\text{WENO}}, \quad \mathbf{V}_{j+\frac{1}{2}}^{n,(1)} = \frac{\mathbf{V}_{j+1}^{\text{WENO}} - \mathbf{V}_j^{\text{WENO}}}{\Delta x}, \quad \mathbf{V}_{j+\frac{1}{2}}^{n,(2)} = \frac{12(\mathbf{V}_{j+\frac{1}{2}}^{\text{WENO}} - \bar{\mathbf{V}}_{j+\frac{1}{2}}^n)}{\Delta x^2},$$

where $\mathbf{V}_{j+\frac{1}{2}}^{\text{WENO}} := \frac{1}{2}(\mathbf{V}_j^{\text{WENO}} + \mathbf{V}_{j+1}^{\text{WENO}})$, $\mathbf{V}_j^{\text{WENO}} := \mathbf{R}_{j+1/2} \mathbf{W}_j^{\text{WENO}}$, $\mathbf{R}_{j+1/2}$ denotes the right eigenvector matrix of $\mathbf{A}(\bar{\mathbf{V}}_{j+1/2}^n)$ and $\mathbf{W}_j^{\text{WENO}}$ is obtained by using the fifth-order accurate WENO reconstruction to the data $\{\bar{\mathbf{W}}_{j+1/2}^n := \mathbf{R}_{j+1/2}^{-1} \bar{\mathbf{V}}_{j+1/2}^n\}$.

3.2. Resolution of the generalised Riemann problem

We now begin to resolve the local GRP for (2.1) with the initial data (3.5), in order to get the approximate states $\mathbf{V}_j^{n+1/2}$ and $\mathbf{V}_j^{n+1,-}$ in (3.3). For convenience, the subscript j and the superscript n will be ignored, and the local GRP for (2.1) with (3.5) transformed via a translation transformation $\{(x - x_j, t - t_n) \mapsto (x, t)\}$ to the “non-local” GRP for (2.1) with the initial data

$$U(x, 0) = \begin{cases} U_L + xU'_L + \frac{1}{2}x^2U''_L, & x < 0, \\ U_R + xU'_R + \frac{1}{2}x^2U''_R, & x > 0, \end{cases} \quad (3.6)$$

where $U_L, U_R, U'_L, U'_R, U''_L$ and U''_R are corresponding known vectors. The limiting value at $x = j$ as $t \rightarrow t_n^+$ will be denoted $(\bullet)_j^n$, on introducing the notation $(\bullet)_*$.

The local wave configuration around the singular point $(x, t) = (0, 0)$ of the GRP for (2.1) with (3.6) only depends on six known vectors in (3.6), and is usually piecewise smooth with finitely many noninteracting rarefaction or shock waves, or contact discontinuities. A local wave configuration with a left-moving rarefaction wave, a contact discontinuity and a right-moving shock wave is shown schematically in Fig. 1. The initial structure

of the solution $U^{\text{GRP}}(x, t)$ to the GRP for (2.1) with (3.6) may be determined according to the relation

$$\lim_{t \rightarrow 0^+} U^{\text{GRP}}(t\lambda, t) = U^{\text{RP}}(\lambda; U_L, U_R), \quad x = t\lambda,$$

where $U^{\text{RP}}(x/t; U_L, U_R)$ can be obtained by using the exact Riemann solver in Ref. [11] for the (classical) RP of (2.1) with the initial data

$$U(x, 0) = \begin{cases} U_L, & x < 0, \\ U_R, & x > 0. \end{cases} \quad (3.7)$$

For a comparison, Fig. 2 displays a local wave configuration of the RP for (2.1) with (3.7). In Figs. 1 and 2, α and β denote characteristic coordinates introduced in Section 3.2.1 within the rarefaction wave.

Similar to the second-order accurate GRP scheme in Ref. [21], the approximate states $V_j^{n+1/2}$ and $V_j^{n+1,-}$ in (3.3) will be obtained by using the Rankine-Hugoniot jump conditions or Riemann invariants to resolve the GRP for (2.1) with (3.6) in the Eulerian formulation. For the non-sonic case, in view of (3.4) and the continuity of u and p across the contact discontinuity, the calculation of $V_j^{n+1/2}$ and $V_j^{n+1,-}$ reduces to forming the system of linear algebraic equations

$$\begin{cases} a_L^{(1)} \left(\frac{\mathcal{D}u}{\mathcal{D}t} \right)_* + b_L^{(1)} \left(\frac{\mathcal{D}p}{\mathcal{D}t} \right)_* = d_L^{(1)}, \\ a_R^{(1)} \left(\frac{\mathcal{D}u}{\mathcal{D}t} \right)_* + b_R^{(1)} \left(\frac{\mathcal{D}p}{\mathcal{D}t} \right)_* = d_R^{(1)}, \end{cases} \quad (3.8)$$

in the unknowns $(\mathcal{D}u/\mathcal{D}t)_*$ and $(\mathcal{D}p/\mathcal{D}t)_*$, and the linear system

$$\begin{cases} a_L^{(2)} \left(\frac{\mathcal{D}^2u}{\mathcal{D}t^2} \right)_* + b_L^{(2)} \left(\frac{\mathcal{D}^2p}{\mathcal{D}t^2} \right)_* = d_L^{(2)}, \\ a_R^{(2)} \left(\frac{\mathcal{D}^2u}{\mathcal{D}t^2} \right)_* + b_R^{(2)} \left(\frac{\mathcal{D}^2p}{\mathcal{D}t^2} \right)_* = d_R^{(2)}, \end{cases} \quad (3.9)$$

in the unknowns $(\mathcal{D}^2u/\mathcal{D}t^2)_*$ and $(\mathcal{D}^2p/\mathcal{D}t^2)_*$, by respectively resolving the left and right nonlinear waves in the GRP. Since the derivation of the system (3.8) is similar to that in Ref. [21], we do not repeat that here, and it remains to derive the system (3.9). Specific attention will be paid to the local wave configuration in Fig. 1, but other local wave configurations can be dealt with similarly and are considered in the code.

3.2.1. Resolution of the rarefaction wave

We now resolve the left rarefaction wave shown in Fig. 1 analytically, using the Riemann invariants to derive the first equation in (3.9). Similar to Ref. [21], the region of the left rarefaction wave in Fig. 1 is described by the set $\mathcal{R} := \{(\alpha(x, t), \beta(x, t)) | \beta \in [\beta_L, \beta_*], -\infty \leq \alpha < 0\}$, where $\beta_L := \lambda_-(U_L)$ and $\beta_* := \lambda_-(U_*)$, with $\beta = \beta(x, t)$ the initial value of the slope λ_- at the singular point $(x, t) = (0, 0)$ and $\alpha = \alpha(x, t)$ denoting the ‘‘transversal’’

by solving the initial-value problem

$$\frac{dt}{d\beta} = \frac{t}{u(0, \beta) - \beta}, \quad t(\beta_L) = \alpha\beta_L^{-1},$$

which is formed in view of the relation along the β -curve in Fig. 2

$$\frac{dx}{dt} = \frac{d(\beta t)}{dt} = t \frac{d\beta}{dt} + \beta = u(0, \beta).$$

Both local coordinate transformations within the rarefaction waves in Figs. 1 and 2 satisfy the properties [4]

$$\frac{\partial \lambda_-}{\partial \beta}(0, \beta) = 1, \quad \frac{\partial t}{\partial \alpha}(0, \beta) = \frac{\partial t_{\text{ass}}}{\partial \alpha}(0, \beta), \quad \frac{\partial t}{\partial \beta}(0, \beta) = 0, \quad \beta_L \leq \beta \leq \beta_*, \quad (3.14)$$

and the asymptotic relations [2]

$$t(\alpha, \beta) = t_{\text{ass}}(\alpha, \beta) + \eta(\alpha, \beta)\alpha^2, \quad x(\alpha, \beta) = x_{\text{ass}}(\alpha, \beta) + \epsilon(\alpha, \beta)\alpha^2. \quad (3.15)$$

Due to (3.14), Eq. (3.12) implies

$$\frac{\partial^2 t}{\partial \alpha \partial \beta}(0, \beta) = \frac{1}{\lambda_0(0, \beta) - \lambda_-(0, \beta)} \frac{\partial t}{\partial \alpha}(0, \beta). \quad (3.16)$$

Remark 3.2. For the ideal gas law (2.2), comparing (2.13) to $S(0, \beta) = S_L$ gives

$$K(0, \beta) = \frac{c_s(0, \beta)}{c_{s,L}} K_L. \quad (3.17)$$

In order to derive the first equation in (3.9), we need

$$\frac{\partial S}{\partial x} = \frac{1}{\lambda_- - \lambda_0} \left(\frac{\partial t}{\partial \alpha} \right)^{-1} \frac{\partial S}{\partial \alpha}, \quad (3.18)$$

$$\frac{\partial \psi_-}{\partial x} = \frac{1}{\lambda_- - \lambda_0} \left(\frac{\partial t}{\partial \alpha} \right)^{-1} \left(\frac{\lambda_- - \lambda_0}{\lambda_- - \lambda_+} \frac{\partial \psi_-}{\partial \alpha} - \frac{\lambda_+ - \lambda_0}{\lambda_- - \lambda_+} K \frac{\partial S}{\partial \alpha} \right), \quad (3.19)$$

and the two lemmas given below, where the definitions of the coordinates (α, β) and (2.11) have been used and the last equation is derived from

$$\begin{aligned} \frac{\partial \psi_-}{\partial \alpha} &= \frac{\partial t}{\partial \alpha} \left(\frac{\partial \psi_-}{\partial t} + \lambda_- \frac{\partial \psi_-}{\partial x} \right) = \frac{\partial t}{\partial \alpha} \left((\lambda_+ - \lambda_0) K S_x + (\lambda_- - \lambda_+) \frac{\partial \psi_-}{\partial x} \right) \\ &= \frac{\lambda_+ - \lambda_0}{\lambda_- - \lambda_0} K \frac{\partial S}{\partial \alpha} + (\lambda_- - \lambda_+) \frac{\partial t}{\partial \alpha} \frac{\partial \psi_-}{\partial x}. \end{aligned}$$

Lemma 3.1. For ψ_{\pm} defined in (2.8), the mixed second partial derivatives with respect to α and β are given by

$$\frac{\partial^2 \psi_+}{\partial \alpha \partial \beta} = - \left. \frac{\partial K}{\partial \beta} \frac{\partial S}{\partial \alpha} \right|_{\beta=\beta_L}, \quad (3.20)$$

$$\begin{aligned} \frac{\partial^2 \psi_-}{\partial \alpha \partial \beta} = & \frac{\lambda_+ - \lambda_0}{\lambda_+ - \lambda_-} \frac{\partial t}{\partial \beta} \left(\frac{\partial t}{\partial \alpha} \right)^{-1} \left\{ \frac{\partial^2 \psi_-}{\partial \alpha^2} - \frac{\partial}{\partial \alpha} \left(K \frac{\partial S}{\partial \alpha} \right) - \left(\frac{\partial t}{\partial \alpha} \right)^{-1} \frac{\partial^2 t}{\partial \alpha^2} \left(\frac{\partial \psi_-}{\partial \alpha} - K \frac{\partial S}{\partial \alpha} \right) \right\} \\ & + \left\{ \frac{\lambda_+ - \lambda_0}{\lambda_+ - \lambda_-} \frac{\partial^2 t}{\partial \alpha \partial \beta} + \frac{\partial}{\partial \alpha} \left(\frac{\lambda_+ - \lambda_0}{\lambda_+ - \lambda_-} \right) \frac{\partial t}{\partial \beta} \right\} \left(\frac{\partial t}{\partial \alpha} \right)^{-1} \left(\frac{\partial \psi_-}{\partial \alpha} - K \frac{\partial S}{\partial \alpha} \right). \end{aligned} \quad (3.21)$$

For the ideal gas (2.2), at the point $(0, \beta)$ the above equations reduce to

$$\frac{\partial^2 \psi_+}{\partial \alpha \partial \beta} = - \left. \frac{\partial c_s}{\partial \beta} \frac{K_L}{c_{s,L}} \frac{\partial S}{\partial \alpha} \right|_L, \quad (3.22)$$

$$\frac{\partial^2 \psi_-}{\partial \alpha \partial \beta} = \frac{\gamma^2(1 - uc_s)^2}{2} \left(\left. \frac{1}{c_s} \frac{\partial \psi_-}{\partial \alpha} - \frac{K_L}{c_{s,L}} \frac{\partial S}{\partial \alpha} \right|_L \right), \quad (3.23)$$

which further yield

$$\frac{\partial \psi_+}{\partial \alpha} = - \left. \frac{c_s K_L}{c_{s,L}} \frac{\partial S}{\partial \alpha} \right|_L, \quad (3.24)$$

$$\begin{aligned} \frac{\partial \psi_-}{\partial \alpha} = & \left. \frac{\partial \psi_-}{\partial \alpha} \right|_L \exp \left(\int_{\beta_L}^{\beta} \mathcal{C}_0(\omega) d\omega \right) \\ & - \left. \frac{K_L}{c_{s,L}} \frac{\partial S}{\partial \alpha} \right|_L \int_{\beta_L}^{\beta} \mathcal{C}_0(\omega) c_s(0, \omega) \exp \left(\int_{\omega}^{\beta} \mathcal{C}_0(\hat{\beta}) d\hat{\beta} \right) d\omega \end{aligned} \quad (3.25)$$

on integrating Eq. (3.23) with respect to β , where $\mathcal{C}_0(\beta) = (\gamma^2(1 - uc_s)^2 / (2c)) (0, \beta)$.

Proof. (1). The first equation of (2.3) gives

$$\frac{\partial^{k+1} S}{\partial \alpha^k \partial \beta} = \frac{\partial^k}{\partial \alpha^k} \left(\frac{\partial S}{\partial \beta} \right) = \frac{\partial^k}{\partial \alpha^k} \left(\frac{\partial t}{\partial \beta} \left(\frac{\partial S}{\partial t} + u \frac{\partial S}{\partial x} \right) \right) = 0, \quad \forall k \in \mathcal{N},$$

whence

$$\frac{\partial^k S}{\partial \alpha^k}(\alpha, \beta) = \frac{\partial^k S}{\partial \alpha^k}(\alpha, \beta_L), \quad \forall k \in \mathcal{N}, \quad (3.26)$$

and hence from (2.11) we obtain

$$\frac{\partial \psi_+}{\partial \alpha} = -K \frac{\partial S}{\partial \alpha}(\alpha, \beta_L). \quad (3.27)$$

Differentiating this equation with respect to β gives Eq. (3.20); and for ideal gases, taking $\alpha \rightarrow 0$ in Eq. (3.20) and using Eq. (3.17) gives Eq. (3.22). Eq. (3.27) also yields Eq. (3.24) on setting $\alpha = 0$ and using Eq. (3.17).

(2). Using Eqs. (2.11), (3.18) and (3.19) we obtain

$$\begin{aligned}\frac{\partial \psi_-}{\partial \beta} &= \frac{\partial t}{\partial \beta} \left(\frac{\partial \psi_-}{\partial t} + \lambda_0 \frac{\partial \psi_-}{\partial x} \right) = \frac{\partial t}{\partial \beta} \left((\lambda_+ - \lambda_0) K \frac{\partial S}{\partial x} + (\lambda_0 - \lambda_+) \frac{\partial \psi_-}{\partial x} \right) \\ &= \frac{\lambda_+ - \lambda_0}{\lambda_+ - \lambda_-} \frac{\partial t}{\partial \beta} \left(\frac{\partial t}{\partial \alpha} \right)^{-1} \left(\frac{\partial \psi_-}{\partial \alpha} - K \frac{\partial S}{\partial \alpha} \right),\end{aligned}$$

and differentiating this equation with respect to α gives Eq. (3.21). Taking $\alpha \rightarrow 0$ in Eq. (3.21) and using Eqs. (3.14), (3.16) and (3.17) yields Eq. (3.23).

(3). Finally, we solve the ordinary differential equation (3.23) for $\frac{\partial \psi_-}{\partial \alpha}(0, \beta)$ using the initial data $\frac{\partial \psi_-}{\partial \alpha}(0, \beta_L) = \frac{\partial \psi_-}{\partial \alpha}|_L$ to complete the proof. \square

Lemma 3.2. For $t(\alpha, \beta)$ defined in (3.11), the limiting value of its second partial derivative with respect to α can be expressed as

$$\frac{\partial^2 t}{\partial \alpha^2}(0, \beta) = \left(\frac{\partial^2 t}{\partial \alpha^2} \Big|_L + \int_{\beta_L}^{\beta} A(\hat{\beta}) d\hat{\beta} \right) \exp \left(\int_{\beta_L}^{\beta} \frac{d\hat{\beta}}{\lambda_0(0, \hat{\beta}) - \lambda_-(0, \hat{\beta})} \right) \quad (3.28)$$

where $A(\beta)$ is defined by

$$A(\beta) := \exp \left(- \int_{\beta_L}^{\beta} \frac{d\omega}{\lambda_0(0, \omega) - \lambda_-(0, \omega)} \right) \frac{F(0, \beta)}{\lambda_0(0, \beta) - \lambda_-(0, \beta)}, \quad (3.29)$$

with

$$F(0, \beta) = \left((\lambda_- - \lambda_0)^{-1} \frac{\partial}{\partial \alpha} (2\lambda_0 - \lambda_-) \frac{\partial t}{\partial \alpha} + \frac{\partial^2 \lambda_-}{\partial \alpha \partial \beta} \frac{\partial t}{\partial \alpha} \right) (0, \beta), \quad (3.30)$$

and the respective calculations of $\partial^2 t / \partial \alpha^2|_L$ and $\partial^2 \lambda_- / \partial \alpha \partial \beta$ are presented in Appendices A and B for the ideal gas law (2.2).

Proof. Differentiating Eq. (3.12) with respect to α gives

$$(\lambda_0 - \lambda_-) \frac{\partial^3 t}{\partial \alpha^2 \partial \beta} = F(\alpha, \beta) + \frac{\partial \lambda_-}{\partial \beta} \frac{\partial^2 t}{\partial \alpha^2}, \quad (3.31)$$

where

$$F(\alpha, \beta) := - \frac{\partial (2\lambda_0 - \lambda_-)}{\partial \alpha} \frac{\partial^2 t}{\partial \alpha \partial \beta} - \frac{\partial^2 \lambda_0}{\partial \alpha^2} \frac{\partial t}{\partial \beta} + \frac{\partial^2 \lambda_-}{\partial \alpha \partial \beta} \frac{\partial t}{\partial \alpha}. \quad (3.32)$$

Letting $\alpha \rightarrow 0$ in Eq. (3.32) gives the expression of $F(0, \beta)$ in Eq. (3.29) with Eqs. (3.14) and (3.16). Thus as $\alpha \rightarrow 0$, Eq. (3.31) becomes

$$\frac{\partial^3 t}{\partial \alpha^2 \partial \beta}(0, \beta) = \frac{1}{\lambda_0(0, \beta) - \lambda_-(0, \beta)} \left(F(0, \beta) + \frac{\partial^2 t}{\partial \alpha^2}(0, \beta) \right), \quad (3.33)$$

which can be considered a first-order ordinary differential equation of $\frac{\partial^2 t}{\partial \alpha^2}(0, \beta)$ with the initial data $\frac{\partial^2 t}{\partial \alpha^2}(0, \beta_L) = \frac{\partial^2 t}{\partial \alpha^2}|_L$. Solving Eq. (3.33) gives Eq. (3.28) and completes the proof. \square

With the help of Lemmas 3.1 and 3.2, the first equation in (3.9) derived as follows.

Proposition 3.1. *The limiting values $(\mathcal{D}^2u/\mathcal{D}t^2)_*$ and $(\mathcal{D}^2p/\mathcal{D}t^2)_*$ satisfy*

$$a_L^{(2)} \left(\frac{\mathcal{D}^2u}{\mathcal{D}t^2} \right)_* + b_L^{(2)} \left(\frac{\mathcal{D}^2p}{\mathcal{D}t^2} \right)_* = d_L^{(2)},$$

where

$$a_L^{(2)} = 1, \quad b_L^{(2)} = \Phi_*,$$

in which $d_L^{(2)}$ depends on the initial data $\mathbf{U}_L, \mathbf{U}'_L, \mathbf{U}''_L$ and the limiting values \mathbf{V}_* , $(\partial\mathbf{V}/\partial t)_*$, $(\partial\mathbf{V}/\partial x)_*$ (as expressed in the following proof) and $\Phi := 1/(\rho h \gamma^2 c_s)$.

Proof. Differentiating Eq. (3.21) with respect to α and then setting $\alpha = 0$ gives

$$\frac{\partial^3 \psi_-}{\partial \alpha^2 \partial \beta}(0, \beta) = G(\beta) + \frac{1}{\lambda_0(0, \beta) - \lambda_-(0, \beta)} \frac{\partial^2 \psi_-}{\partial \alpha^2}(0, \beta) \quad (3.34)$$

with

$$G(\beta) = \frac{1}{\lambda_0 - \lambda_-} \left[\frac{1}{2} \left(\frac{\partial t}{\partial \alpha} \right)^{-1} \left(\frac{\partial \psi_-}{\partial \alpha} - K \frac{\partial S}{\partial \alpha} \right) \Big|_L \left(F - \frac{\partial^2 t}{\partial \alpha^2} \right) - \frac{\partial K}{\partial \alpha} \frac{\partial S}{\partial \alpha} \Big|_L - K \frac{\partial^2 S}{\partial \alpha^2} \Big|_L \right] (0, \beta),$$

where Eqs. (3.14), (3.16), (3.33) and (3.26) have all been used here. Referring to (3.26) and Lemma 3.2, we have $\frac{\partial^2 S}{\partial \alpha^2}(0, \beta) = \frac{\partial^2 S}{\partial \alpha^2} \Big|_L$, so $G(\beta)$ depends on the initial data $\mathbf{U}_L, \mathbf{U}'_L, \mathbf{U}''_L$ and the values $\mathbf{V}(0, \beta)$ and $\frac{\partial \mathbf{V}}{\partial \alpha}(0, \beta)$. Integrating Eq. (3.34) with respect to β then gives

$$\frac{\partial^2 \psi_-}{\partial \alpha^2}(0, \beta) = \left(\frac{\partial^2 \psi_-}{\partial \alpha^2} \Big|_L + \int_{\beta_L}^{\beta} C(\hat{\beta}) d\hat{\beta} \right) \exp \left(\int_{\beta_L}^{\beta} \frac{d\hat{\beta}}{\lambda_0(0, \hat{\beta}) - \lambda_-(0, \hat{\beta})} \right) \quad (3.35)$$

with

$$C(\beta) := \exp \left(- \int_{\beta_L}^{\beta} \frac{d\hat{\beta}}{\lambda_0(0, \hat{\beta}) - \lambda_-(0, \hat{\beta})} \right) G(\beta),$$

depending on the initial data $\mathbf{U}_L, \mathbf{U}'_L, \mathbf{U}''_L$ and the limiting values $\mathbf{V}(0, \beta)$, $\frac{\partial \mathbf{V}}{\partial \alpha}(0, \beta)$, and hence $\frac{\partial^2 \psi_-}{\partial \alpha^2}(0, \beta)$ as well.

On the other hand, from (2.9) the second-order derivatives of ψ_-, u and p with respect to α can be expressed as

$$\frac{\partial^2 \psi_-}{\partial \alpha^2} = \frac{\partial}{\partial \alpha} \left(\gamma^2 \frac{\partial u}{\partial \alpha} + \frac{1}{\rho h c_s} \frac{\partial p}{\partial \alpha} + K \frac{\partial S}{\partial \alpha} \right) = \gamma^2 \left(\frac{\partial^2 u}{\partial \alpha^2} + \Phi \frac{\partial^2 p}{\partial \alpha^2} \right) + \Xi_\psi \quad (3.36)$$

and

$$\frac{\partial^2 u}{\partial \alpha^2} = \frac{2}{(1 - u c_s)^2} \left(\frac{\partial t}{\partial \alpha} \right)^2 \left(\frac{\mathcal{D}^2 u}{\mathcal{D} t^2} + \Phi \frac{\mathcal{D}^2 p}{\mathcal{D} t^2} \right) + \Xi_u, \quad (3.37)$$

$$\frac{\partial^2 p}{\partial \alpha^2} = \frac{2}{(1 - u c_s)^2} \left(\frac{\partial t}{\partial \alpha} \right)^2 \left(\Phi^{-1} \frac{\mathcal{D}^2 u}{\mathcal{D} t^2} + \frac{\mathcal{D}^2 p}{\mathcal{D} t^2} \right) + \Xi_p, \quad (3.38)$$

where

$$\begin{aligned}\Xi_\psi &= \frac{\partial \gamma^2}{\partial \alpha} \frac{\partial u}{\partial \alpha} + \frac{\partial}{\partial \alpha} \left(\frac{1}{\rho h c_s} \right) \frac{\partial p}{\partial \alpha} + \frac{\partial K}{\partial \alpha} \frac{\partial S}{\partial \alpha} \Big|_{\beta=\beta_L} + K \frac{\partial^2 S}{\partial \alpha^2} \Big|_{\beta=\beta_L}, \\ \Xi_u &= \left[\frac{1}{1-uc_s} \frac{\partial^2 t}{\partial \alpha^2} + \frac{\partial t}{\partial \alpha} \frac{\partial(1-uc_s)^{-1}}{\partial \alpha} \right] \left(\frac{\mathcal{D}u}{\mathcal{D}t} + \Phi \frac{\mathcal{D}p}{\mathcal{D}t} \right) + \frac{1}{1-uc_s} \left(\frac{\partial t}{\partial \alpha} \right)^2 \frac{\mathcal{D}\Phi}{\mathcal{D}t} \frac{\mathcal{D}p}{\mathcal{D}t} \\ &\quad + \frac{\lambda_0 - \lambda_-}{1-uc_s} \left(\frac{\partial t}{\partial \alpha} \right)^2 \left[- \left(\frac{\partial \Phi}{\partial x} \frac{\mathcal{D}p}{\mathcal{D}t} + \left(\frac{\partial u}{\partial x} \right)^2 + \Phi \frac{\partial u}{\partial x} \frac{\partial p}{\partial x} \right) \right. \\ &\quad \left. + \left(\frac{\mathcal{D}(\gamma^2 u)}{\mathcal{D}t} + \Phi \frac{\mathcal{D}(\rho h \gamma^4)}{\mathcal{D}t} \right) \frac{\mathcal{D}u}{\mathcal{D}t} + \left(\frac{\mathcal{D}(\rho h c_s^2)^{-1}}{\mathcal{D}t} + \Phi \frac{\mathcal{D}(\gamma^2 u)}{\mathcal{D}t} \right) \frac{\mathcal{D}p}{\mathcal{D}t} \right], \\ \Xi_p &= \Phi^{-1} \Xi_u + \frac{1}{1-uc_s} \left(\frac{\partial t}{\partial \alpha} \right)^2 \left(\frac{\partial \Phi}{\partial t} + \lambda_- \frac{\partial \Phi}{\partial x} \right) \left(\frac{\mathcal{D}u}{\mathcal{D}t} + \Phi \frac{\mathcal{D}p}{\mathcal{D}t} \right).\end{aligned}$$

Substituting Eqs. (3.35), (3.37) and (3.38) into Eq. (3.36) and setting $\alpha = 0$ and $\beta = \beta_*$ gives

$$a_L^{(2)} = 1, \quad b_L^{(2)} = \Phi_*$$

and

$$d_L^{(2)} = \frac{(1-uc_s)_*^2}{4} \left(\frac{\partial t}{\partial \alpha} \right)_*^{-2} \left(\gamma^{-2} \left(\frac{\partial^2 \psi_-}{\partial \alpha^2} - \Xi_\psi \right) - \Xi_u - \Phi \Xi_p \right)_*,$$

with $(\partial^2 \psi_- / \partial \alpha^2)_*$ obtained by setting $\beta = \beta_*$ in Eq. (3.35). Since $(\partial^2 t / \partial \alpha^2)_*$ only depends on the initial data U_L, U'_L, U''_L and the limiting values V_* and $(\partial V / \partial \alpha)_*$, $d_L^{(2)}$ depends on the initial data U_L, U'_L, U''_L and the limiting values $V_*, (V_t)_*, (V_x)_*$, so the proof is complete. \square

Remark 3.3. If the right rarefaction wave associated with the eigenvalue λ_+ appears in the GRP, then under the “reflective symmetry” transformation

$$\rho(x, t) = \tilde{\rho}(-x, t), \quad u(x, t) = -\tilde{u}(-x, t), \quad p(x, t) = \tilde{p}(-x, t),$$

where $(\rho, u, p)^T$ and $(\tilde{\rho}, \tilde{u}, \tilde{p})^T$ denote the respective primitive variables before and after the reflective transformation, the above derivation can be used. (The “reflective symmetry” transformation maps the “real” right rarefaction wave into a “virtual” left rarefaction wave, so Proposition 3.1 is directly applied to the “virtual” left rarefaction wave, and finally the inverse transformation gives the linear equation in $(\mathcal{D}^2 u / \mathcal{D}t^2)_*$ and $(\mathcal{D}^2 p / \mathcal{D}t^2)_*$ for the right rarefaction wave.)

3.2.2. Resolution of the shock waves

In this section, we resolve the right shock wave in Fig. 1 analytically using the Rankine-Hugoniot jump conditions, and obtain the second equation in (3.9).

Let the shock trajectory associated with the eigenvalue λ_+ be denoted by $x = x_s(t)$ with the positive speed $s := d/dt x_s(t) > 0$ (for convenience), and the left and right states

of the shock wave by $U(t)$ and $\bar{U}(t)$, respectively — i.e. $U(t) = U(x_s(t) - 0, t)$ and $\bar{U}(t) = U(x_s(t) + 0, t)$. Obviously, $\bar{U}(0) = U_R$, and the left and right states satisfy

$$\left(\frac{\bar{u} - u}{1 - u\bar{u}} \right)^2 = \Psi(p, \mu; \bar{p}, \bar{\mu}), \quad p > \bar{p}, \quad (3.39)$$

with $\mu := \rho + \rho e$ and

$$\Psi(p, \mu; \bar{p}, \bar{\mu}) := \frac{(p - \bar{p})(\mu - \bar{\mu})}{(\bar{\mu} + p)(\mu + \bar{p})}$$

derived from the Rankine–Hugoniot jump conditions across the right shock wave, where $p > \bar{p}$ and $u > \bar{u}$. Introducing the directional derivative operators along the shock trajectory

$$\frac{\mathcal{D}_s}{\mathcal{D}t} := \frac{\partial}{\partial t} + s \frac{\partial}{\partial x} = \frac{\mathcal{D}}{\mathcal{D}t} + (s - u) \frac{\partial}{\partial x}, \quad s = \frac{\rho\gamma u - \bar{\rho}\bar{\gamma}\bar{u}}{\rho\gamma - \bar{\rho}\bar{\gamma}},$$

one has

$$\frac{\mathcal{D}_s^2 u}{\mathcal{D}t^2} = \gamma^4 \left[(1 - us)^2 + c_s^{-2}(u - s)^2 \right] \frac{\mathcal{D}^2 u}{\mathcal{D}t^2} + 2 \frac{u - s}{\rho h c_s^2} \gamma^2 (1 - us) \frac{\mathcal{D}^2 p}{\mathcal{D}t^2} + \Pi_u, \quad (3.40)$$

$$\frac{\mathcal{D}_s^2 p}{\mathcal{D}t^2} = 2\rho h \gamma^6 (1 - us)(u - s) \frac{\mathcal{D}^2 u}{\mathcal{D}t^2} + \gamma^4 \left[(1 - us)^2 + c_s^{-2}(u - s)^2 \right] \frac{\mathcal{D}^2 p}{\mathcal{D}t^2} + \Pi_p, \quad (3.41)$$

where (2.4) has been used within the smooth region at the right-hand or left-hand side of the shock wave, and

$$\begin{aligned} \Pi_u &= (u - s) \left[\frac{1 - us}{1 - u^2} \frac{\mathcal{D}}{\mathcal{D}t} (\gamma^2 u) + \frac{u - s}{\rho h c_s^2} \frac{\mathcal{D}}{\mathcal{D}t} (\rho h \gamma^4) \right] \frac{\mathcal{D}u}{\mathcal{D}t} \\ &\quad + (u - s) \left[\frac{1 - us}{1 - u^2} \frac{\mathcal{D}}{\mathcal{D}t} (\rho h c_s^2)^{-1} + \frac{u - s}{\rho h c_s^2} \frac{\mathcal{D}}{\mathcal{D}t} (u \gamma^2) \right] \frac{\mathcal{D}p}{\mathcal{D}t} \\ &\quad - (u - s) \left[\frac{1 - us}{1 - u^2} \frac{\partial u}{\partial x} + \frac{u - s}{\rho h c_s^2} \frac{\partial p}{\partial x} \right] \frac{\partial u}{\partial x} + \frac{\mathcal{D}_s}{\mathcal{D}t} \left(\frac{u - s}{1 - u^2} \right) \frac{\mathcal{D}u}{\mathcal{D}t} + \frac{\mathcal{D}_s}{\mathcal{D}t} \left(\frac{u - s}{\rho h c_s^2} \right) \frac{\mathcal{D}p}{\mathcal{D}t}, \\ \Pi_p &= (u - s) \gamma^2 \left[\rho h \gamma^2 (u - s) \frac{\mathcal{D}}{\mathcal{D}t} (\gamma^2 u) + (1 - us) \frac{\mathcal{D}}{\mathcal{D}t} (\rho h \gamma^4) \right] \frac{\mathcal{D}u}{\mathcal{D}t} \\ &\quad + (u - s) \gamma^2 \left[\rho h \gamma^2 (u - s) \frac{\mathcal{D}}{\mathcal{D}t} (\rho h c_s^2)^{-1} + (1 - us) \frac{\mathcal{D}}{\mathcal{D}t} (\gamma^2 u) \right] \frac{\mathcal{D}p}{\mathcal{D}t} \\ &\quad - (u - s) \gamma^2 \left[\rho h \gamma^2 (u - s) \frac{\partial u}{\partial x} + (1 - us) \frac{\partial p}{\partial x} \right] \frac{\partial u}{\partial x} \\ &\quad + \frac{\mathcal{D}_s}{\mathcal{D}t} \left(\rho h \gamma^4 (u - s) \right) \frac{\mathcal{D}u}{\mathcal{D}t} + \frac{\mathcal{D}_s}{\mathcal{D}t} \left(\gamma^2 (1 - us) \right) \frac{\mathcal{D}p}{\mathcal{D}t}. \end{aligned}$$

The second equation in (3.9) may be derived as follows.

Proposition 3.2. *The limiting values of $(\mathcal{D}^2 u / \mathcal{D}t^2)_*$ and $(\mathcal{D}^2 p / \mathcal{D}t^2)_*$ satisfy*

$$a_R^{(2)} \left(\frac{\mathcal{D}^2 u}{\mathcal{D}t^2} \right)_* + b_R^{(2)} \left(\frac{\mathcal{D}^2 p}{\mathcal{D}t^2} \right)_* = d_R^{(2)}, \quad (3.42)$$

where the coefficients $a_R^{(2)}, b_R^{(2)}$ depend on the initial data \mathbf{U}_R and the limiting values $\mathbf{V}_*, d_R^{(2)}$ dependent on the initial data $\mathbf{U}_R, \mathbf{U}'_R, \mathbf{U}''_R$ and the limiting values $\mathbf{V}_*, (\mathbf{V}_t)_*, (\mathbf{V}_x)_*$. Their expressions are given in the following proof.

Proof. The operation $\mathcal{D}_s^2/\mathcal{D}t^2$ on the shock relation (3.39) gives

$$\frac{\mathcal{D}_s^2}{\mathcal{D}t^2} \left(\frac{\bar{u} - u}{1 - \bar{u}u} \right)^2 = \frac{\mathcal{D}_s^2}{\mathcal{D}t^2} \Psi(p, \mu, \bar{p}, \bar{\mu}), \quad (3.43)$$

where the left-hand and right-hand sides can be respectively expanded as follows:

$$\text{LHS(3.43)} = \frac{2(\bar{u} - u)(\bar{u}^2 - 1)}{(1 - \bar{u}u)^3} \frac{\mathcal{D}_s^2 u}{\mathcal{D}t^2} + \Pi_{\bar{u}u} \quad (3.44)$$

with

$$\Pi_{\bar{u}u} := \frac{2(\bar{u} - u)}{1 - \bar{u}u} \left[\frac{\mathcal{D}_s}{\mathcal{D}t} \left(\frac{\frac{\mathcal{D}_s \bar{u}}{\mathcal{D}t} (1 - u^2)}{(1 - \bar{u}u)^2} \right) + \frac{\mathcal{D}_s}{\mathcal{D}t} \left(\frac{\bar{u}^2 - 1}{(1 - \bar{u}u)^2} \right) \frac{\mathcal{D}_s u}{\mathcal{D}t} \right] + 2 \left[\frac{\mathcal{D}_s}{\mathcal{D}t} \left(\frac{\bar{u} - u}{1 - \bar{u}u} \right) \right]^2;$$

and

$$\begin{aligned} \text{RHS(3.43)} = & \Psi_\mu \frac{\mathcal{D}_s^2 \mu}{\mathcal{D}t^2} + \Psi_p \frac{\mathcal{D}_s^2 p}{\mathcal{D}t^2} + \Psi_{\bar{\mu}} \frac{\mathcal{D}_s^2 \bar{\mu}}{\mathcal{D}t^2} + \Psi_{\bar{p}} \frac{\mathcal{D}_s^2 \bar{p}}{\mathcal{D}t^2} \\ & + \frac{\mathcal{D}_s \Psi_\mu}{\mathcal{D}t} \frac{\mathcal{D}_s \mu}{\mathcal{D}t} + \frac{\mathcal{D}_s \Psi_p}{\mathcal{D}t} \frac{\mathcal{D}_s p}{\mathcal{D}t} + \frac{\mathcal{D}_s \Psi_{\bar{\mu}}}{\mathcal{D}t} \frac{\mathcal{D}_s \bar{\mu}}{\mathcal{D}t} + \frac{\mathcal{D}_s \Psi_{\bar{p}}}{\mathcal{D}t} \frac{\mathcal{D}_s \bar{p}}{\mathcal{D}t}, \end{aligned} \quad (3.45)$$

where

$$\begin{aligned} \frac{\mathcal{D}_s \Psi_\mu}{\mathcal{D}t} &= \frac{(p - \bar{p})^2}{(\bar{\mu} + p)^2 (\mu + \bar{p})^2} \frac{\mathcal{D}_s \bar{\mu}}{\mathcal{D}t} + \frac{(p - \bar{p})(\mu - \bar{\mu}) - \bar{\rho} \bar{h} \rho h}{(\bar{\mu} + p)(\mu + \bar{p})^3} \frac{\mathcal{D}_s \bar{p}}{\mathcal{D}t} \\ &\quad + \frac{2\bar{\rho} \bar{h} (\bar{p} - p)}{(\bar{\mu} + p)(\mu + \bar{p})^3} \frac{\mathcal{D}_s \mu}{\mathcal{D}t} + \frac{(\bar{\rho} \bar{h})^2}{(\bar{\mu} + p)^2 (\mu + \bar{p})^2} \frac{\mathcal{D}_s \bar{p}}{\mathcal{D}t}, \\ \frac{\mathcal{D}_s \Psi_p}{\mathcal{D}t} &= \frac{(p - \bar{p})(\mu - \bar{\mu}) - \bar{\rho} \bar{h} \rho h}{(\bar{\mu} + p)^3 (\mu + \bar{p})} \frac{\mathcal{D}_s \bar{\mu}}{\mathcal{D}t} + \frac{(\mu - \bar{\mu})^2}{(\bar{\mu} + p)^2 (\mu + \bar{p})^2} \frac{\mathcal{D}_s \bar{p}}{\mathcal{D}t} \\ &\quad + \frac{(\bar{\rho} \bar{h})^2}{(\bar{\mu} + p)^2 (\mu + \bar{p})^2} \frac{\mathcal{D}_s \mu}{\mathcal{D}t} + \frac{2\bar{\rho} \bar{h} (\bar{\mu} - \mu)}{(\bar{\mu} + p)^3 (\mu + \bar{p})} \frac{\mathcal{D}_s p}{\mathcal{D}t}, \\ \frac{\mathcal{D}_s \Psi_{\bar{\mu}}}{\mathcal{D}t} &= \frac{2\rho h (p - \bar{p})}{(\bar{\mu} + p)^3 (\mu + \bar{p})} \frac{\mathcal{D}_s \bar{\mu}}{\mathcal{D}t} + \frac{(\rho h)^2}{(\bar{\mu} + p)^2 (\mu + \bar{p})^2} \frac{\mathcal{D}_s \bar{p}}{\mathcal{D}t} \\ &\quad + \frac{(\bar{p} - p)^2}{(\bar{\mu} + p)^2 (\mu + \bar{p})^2} \frac{\mathcal{D}_s \mu}{\mathcal{D}t} + \frac{(p - \bar{p})(\mu - \bar{\mu}) - \bar{\rho} \bar{h} \rho h}{(\bar{\mu} + p)^3 (\mu + \bar{p})} \frac{\mathcal{D}_s p}{\mathcal{D}t}, \\ \frac{\mathcal{D}_s \Psi_{\bar{p}}}{\mathcal{D}t} &= \frac{(\rho h)^2}{(\bar{\mu} + p)^2 (\mu + \bar{p})^2} \frac{\mathcal{D}_s \bar{\mu}}{\mathcal{D}t} + \frac{2\rho h (\mu - \bar{\mu})}{(\bar{\mu} + p)(\mu + \bar{p})^3} \frac{\mathcal{D}_s \bar{p}}{\mathcal{D}t} \\ &\quad + \frac{(p - \bar{p})(\mu - \bar{\mu}) - \bar{\rho} \bar{h} \rho h}{(\bar{\mu} + p)(\mu + \bar{p})^3} \frac{\mathcal{D}_s \mu}{\mathcal{D}t} + \frac{(\bar{\mu} - \mu)^2}{(\bar{\mu} + p)^2 (\mu + \bar{p})^2} \frac{\mathcal{D}_s p}{\mathcal{D}t}. \end{aligned}$$

On considering h as a function of ρ and p (i.e. $h = h(\rho, p)$), we have [21]

$$\begin{cases} \frac{\mathcal{D}_s \rho}{\mathcal{D}t} = \frac{C_{\rho 2}}{C_{\rho 1}} \frac{\mathcal{D}_s p}{\mathcal{D}t} + \frac{C_{\rho 3}}{C_{\rho 1}} \frac{\mathcal{D}_s \bar{\rho}}{\mathcal{D}t} + \frac{C_{\rho 4}}{C_{\rho 1}} \frac{\mathcal{D}_s \bar{p}}{\mathcal{D}t}, \\ \frac{\mathcal{D}_s h}{\mathcal{D}t} = \left(\frac{\partial h}{\partial \rho} \frac{C_{\rho 2}}{C_{\rho 1}} + \frac{\partial h}{\partial p} \right) \frac{\mathcal{D}_s p}{\mathcal{D}t} + \frac{\partial h}{\partial \rho} \left(\frac{C_{\rho 3}}{C_{\rho 1}} \frac{\mathcal{D}_s \bar{\rho}}{\mathcal{D}t} + \frac{C_{\rho 4}}{C_{\rho 1}} \frac{\mathcal{D}_s \bar{p}}{\mathcal{D}t} \right), \end{cases} \quad (3.46)$$

where

$$\begin{cases} C_{\rho 1} = \bar{\rho}(h^2 - \bar{h}^2) - \bar{h}(p - \bar{p}) + \bar{\rho}(2\rho h - p + \bar{p}) \frac{\partial h}{\partial \rho}, \\ C_{\rho 2} = (h\bar{\rho} + \bar{h}\rho) + \bar{\rho}(p - \bar{p} - 2\rho h) \frac{\partial h}{\partial p}, \\ C_{\rho 3} = -\rho(h^2 - \bar{h}^2) + h(p - \bar{p}) + \rho(2\bar{\rho}\bar{h} + p - \bar{p}) \frac{\partial \bar{h}}{\partial \bar{\rho}}, \\ C_{\rho 4} = -(h\bar{\rho} + \bar{h}\rho) + \rho(2\bar{\rho}\bar{h} + p - \bar{p}) \frac{\partial \bar{h}}{\partial \bar{p}}. \end{cases}$$

The relation $\mu = \rho + \rho e = \rho h - p$ yields

$$\frac{\mathcal{D}_s^2 \mu}{\mathcal{D}t^2} = h \frac{\mathcal{D}_s^2 \rho}{\mathcal{D}t^2} + \rho \frac{\mathcal{D}_s^2 h}{\mathcal{D}t^2} + 2 \frac{\mathcal{D}_s \rho}{\mathcal{D}t} \frac{\mathcal{D}_s h}{\mathcal{D}t} - \frac{\mathcal{D}_s^2 p}{\mathcal{D}t^2}. \quad (3.47)$$

The differential operator $\mathcal{D}_s/\mathcal{D}t$ applied to the two equations in (3.46) yield the respective expressions of $\mathcal{D}_s^2 \rho/\mathcal{D}t^2$ and $\mathcal{D}_s^2 h/\mathcal{D}t^2$, and then substituting these expressions into Eq. (3.47) gives

$$\frac{\mathcal{D}_s^2 \mu}{\mathcal{D}t^2} = \left[\frac{C_{\rho 2}}{C_{\rho 1}} \left(h + \rho \frac{\partial h}{\partial \rho} \right) + \rho \frac{\partial h}{\partial p} - 1 \right] \frac{\mathcal{D}_s^2 p}{\mathcal{D}t^2} + \Pi_\mu, \quad (3.48)$$

where

$$\begin{aligned} \Pi_\mu = & 2 \frac{\mathcal{D}_s \rho}{\mathcal{D}t} \frac{\mathcal{D}_s h}{\mathcal{D}t} + h \frac{\mathcal{D}_s}{\mathcal{D}t} \left(\frac{C_{\rho 2}}{C_{\rho 1}} \right) \frac{\mathcal{D}_s p}{\mathcal{D}t} + h \frac{\mathcal{D}_s}{\mathcal{D}t} \left[\frac{C_{\rho 3}}{C_{\rho 1}} \frac{\mathcal{D}_s \bar{\rho}}{\mathcal{D}t} + \frac{C_{\rho 4}}{C_{\rho 1}} \frac{\mathcal{D}_s \bar{p}}{\mathcal{D}t} \right] \\ & + \rho \frac{\mathcal{D}_s}{\mathcal{D}t} \left(\frac{\partial h}{\partial \rho} \frac{C_{\rho 2}}{C_{\rho 1}} + \frac{\partial h}{\partial p} \right) + \rho \frac{\mathcal{D}_s}{\mathcal{D}t} \left[\frac{\partial h}{\partial \rho} \left(\frac{C_{\rho 3}}{C_{\rho 1}} \frac{\mathcal{D}_s \bar{\rho}}{\mathcal{D}t} + \frac{C_{\rho 4}}{C_{\rho 1}} \frac{\mathcal{D}_s \bar{p}}{\mathcal{D}t} \right) \right]. \end{aligned}$$

Substituting Eqs. (3.44) and (3.45) into Eq. (3.43), from Eq. (3.48) for $\mathcal{D}_s^2 \mu/\mathcal{D}t^2$ we have

$$\Pi_{u0} \frac{\mathcal{D}_s^2 u}{\mathcal{D}t^2} + \Pi_{\bar{u}u} = \Pi_{p0} \frac{\mathcal{D}_s^2 p}{\mathcal{D}t^2} + \Pi_\Psi, \quad (3.49)$$

where

$$\Pi_{u0} = \frac{2(\bar{u} - u)(\bar{u}^2 - 1)}{(1 - \bar{u}u)^3},$$

$$\Pi_{p0} = \left[\frac{C_{\rho 2}}{C_{\rho 1}} \left(h + \rho \frac{\partial h}{\partial \rho} \right) + \rho \frac{\partial h}{\partial p} - 1 \right] \Psi_\mu + \Psi_p,$$

$$\Pi_\Psi = \Psi_\mu \Pi_\mu + \Psi_{\bar{\mu}} \frac{\mathcal{D}_s^2 \bar{\mu}}{\mathcal{D}t^2} + \Psi_{\bar{p}} \frac{\mathcal{D}_s^2 \bar{p}}{\mathcal{D}t^2} + \frac{\mathcal{D}_s \Psi_\mu}{\mathcal{D}t} \frac{\mathcal{D}_s \mu}{\mathcal{D}t} + \frac{\mathcal{D}_s \Psi_p}{\mathcal{D}t} \frac{\mathcal{D}_s p}{\mathcal{D}t} + \frac{\mathcal{D}_s \Psi_{\bar{\mu}}}{\mathcal{D}t} \frac{\mathcal{D}_s \bar{\mu}}{\mathcal{D}t} + \frac{\mathcal{D}_s \Psi_{\bar{p}}}{\mathcal{D}t} \frac{\mathcal{D}_s \bar{p}}{\mathcal{D}t}.$$

Finally, substituting (3.40) and (3.41) into (3.49) and then taking $x = 0$ and $t \rightarrow 0^+$, we obtain the identity (3.42) with the coefficients

$$\begin{aligned} a_R^{(2)} &= \left(\gamma^4 \left((1-us)^2 + c_s^{-2}(u-s)^2 \right) \Pi_{u0} - 2\rho h \gamma^6 (1-us)(u-s) \Pi_{p0} \right)_*, \\ b_R^{(2)} &= \left(2 \frac{u-s}{\rho h c_s^2} \gamma^2 (1-us) \Pi_{u0} - \gamma^4 \left[(1-us)^2 + c_s^{-2}(u-s)^2 \right] \Pi_{p0} \right)_*, \\ d_R^{(2)} &= (\Pi_p \Pi_{p0} - \Pi_u \Pi_{u0} + \Pi_\Psi - \Pi_{\bar{u}u})_*, \end{aligned}$$

to complete the proof. \square

Remark 3.4. For the ideal gas, we have explicitly

$$\frac{\partial h}{\partial \rho} = -\frac{\Gamma}{\Gamma-1} \frac{p}{\rho^2}, \quad \frac{\partial h}{\partial p} = \frac{\Gamma}{\Gamma-1} \frac{1}{\rho},$$

when the coefficients $a_R^{(2)}$, $b_R^{(2)}$ and $d_R^{(2)}$ in the above lemma can be calculated readily.

Remark 3.5. If the left shock wave associated with the eigenvalue λ_- appears in the GRP, Proposition 3.2 may first be applied to the “virtual” right shock wave obtained by again using the “reflective symmetry” transformation given in Remark 3.3, and then the corresponding inverse transformation to obtain the linear equation of the limiting values $(\mathcal{D}^2 u / \mathcal{D} t^2)_*$ and $(\mathcal{D}^2 p / \mathcal{D} t^2)_*$.

3.2.3. Approximate flux states in the GRP scheme

Let us now complete the calculation of $V_j^{n+1/2}$ and $V_j^{n+1,-}$ in (3.3), case by case. For the non-sonic case, we require $(V_{tt})_*$ due to (3.4), given in Theorems 3.1 and 3.2. For the sonic case, $V_j^{n+1/2}$ and $V_j^{n+1,-}$ will be derived differently, without using $(V_{tt})_*$.

I. Non-sonic case

The rarefaction wave in Fig. 1 is non-sonic — i.e. $\lambda_-(V_*) < 0$. The calculation of the time derivatives $(u_{tt})_*$ and $(p_{tt})_*$ is via the following theorem for the values $(\mathcal{D}^2 u / \mathcal{D} t^2)_*$ and $(\mathcal{D}^2 p / \mathcal{D} t^2)_*$, which are the solutions of the linear system (3.9) derived from Propositions 3.1 and 3.2.

Theorem 3.1. Assume that the shock speed s is greater than 0. The limiting values of time derivatives $(u_{tt})_*$ and $(p_{tt})_*$ are calculated from the 2×2 linear system

$$\begin{cases} A_0(u_{tt})_* + A_u(p_{tt})_* = \left(\frac{\mathcal{D}^2 u}{\mathcal{D} t^2} \right)_* - D_u, \\ A_p(u_{tt})_* + A_0(p_{tt})_* = \left(\frac{\mathcal{D}^2 p}{\mathcal{D} t^2} \right)_* - D_p, \end{cases} \quad (3.50)$$

where the coefficients

$$A_0 = ((1 + u\Theta_0)^2 + u^2\Theta_u\Theta_p)_*, \quad A_u = (2u\Theta_u(1 + u\Theta_0))_*, \quad A_p = (2u\Theta_p(1 + u\Theta_0))_*$$

depend on V_* ,

$$\Theta_0 := -(2\lambda_+\lambda_-)^{-1}(\lambda_+ + \lambda_-), \quad \Theta_u := (2\lambda_+\lambda_-)^{-1}(\lambda_+ - \lambda_-)\Phi, \quad \Theta_p := \Phi^{-2}\Theta_u$$

and

$$\begin{aligned} D_u &= u_* \left[2\frac{\partial\Theta_0}{\partial t} + u \left(\Theta_u \frac{\partial\Theta_p}{\partial t} + \Theta_0 \frac{\partial\Theta_0}{\partial t} + \frac{\partial\Theta_0}{\partial x} \right) \right]_* \left(\frac{\partial u}{\partial t} \right)_* \\ &\quad + u_* \left[2\frac{\partial\Theta_u}{\partial t} + u \left(\Theta_u \frac{\partial\Theta_0}{\partial t} + \Theta_0 \frac{\partial\Theta_u}{\partial t} + \frac{\partial\Theta_u}{\partial x} \right) \right]_* \left(\frac{\partial p}{\partial t} \right)_* + \left(\frac{\mathcal{D}u}{\mathcal{D}t} \frac{\partial u}{\partial x} \right)_*, \\ D_p &= u_* \left[2\frac{\partial\Theta_p}{\partial t} + u \left(\Theta_p \frac{\partial\Theta_0}{\partial t} + \Theta_0 \frac{\partial\Theta_p}{\partial t} + \frac{\partial\Theta_p}{\partial x} \right) \right]_* \left(\frac{\partial u}{\partial t} \right)_* \\ &\quad + u_* \left[2\frac{\partial\Theta_0}{\partial t} + u \left(\Theta_p \frac{\partial\Theta_u}{\partial t} + \Theta_0 \frac{\partial\Theta_0}{\partial t} + \frac{\partial\Theta_0}{\partial x} \right) \right]_* \left(\frac{\partial p}{\partial t} \right)_* + \left(\frac{\mathcal{D}u}{\mathcal{D}t} \frac{\partial p}{\partial x} \right)_* \end{aligned}$$

rely on V_* , $(V_t)_*$ and $(V_x)_*$. Here V_* and $(V_t)_*$ can be obtained using a procedure for the second-order accurate GRP scheme similar to that in Ref. [21], while $(V_x)_*$ can be calculated using (2.5).

Proof. The second and third equations of (2.3) can be rewritten as

$$\begin{cases} \frac{\partial u}{\partial x} = \Theta_0 \frac{\partial u}{\partial t} + \Theta_u \frac{\partial p}{\partial t}, \\ \frac{\partial p}{\partial x} = \Theta_p \frac{\partial u}{\partial t} + \Theta_0 \frac{\partial p}{\partial t}. \end{cases}$$

Taking partial derivatives with respect to t and x respectively gives

$$\begin{aligned} \frac{\partial^2 u}{\partial t \partial x} &= \Theta_0 \frac{\partial^2 u}{\partial t^2} + \Theta_u \frac{\partial^2 p}{\partial t^2} + \frac{\partial\Theta_0}{\partial t} \frac{\partial u}{\partial t} + \frac{\partial\Theta_u}{\partial t} \frac{\partial p}{\partial t}, \\ \frac{\partial^2 p}{\partial t \partial x} &= \Theta_p \frac{\partial^2 u}{\partial t^2} + \Theta_0 \frac{\partial^2 p}{\partial t^2} + \frac{\partial\Theta_p}{\partial t} \frac{\partial u}{\partial t} + \frac{\partial\Theta_0}{\partial t} \frac{\partial p}{\partial t} \end{aligned} \quad (3.51)$$

and

$$\begin{aligned} \frac{\partial^2 u}{\partial x^2} &= (\Theta_0^2 + \Theta_u\Theta_p) \frac{\partial^2 u}{\partial t^2} + 2\Theta_0\Theta_u \frac{\partial^2 p}{\partial t^2} \\ &\quad + \left(\Theta_u \frac{\partial\Theta_p}{\partial t} + \Theta_0 \frac{\partial\Theta_0}{\partial t} + \frac{\partial\Theta_0}{\partial x} \right) \frac{\partial u}{\partial t} + \left(\Theta_u \frac{\partial\Theta_0}{\partial t} + \Theta_0 \frac{\partial\Theta_u}{\partial t} + \frac{\partial\Theta_u}{\partial x} \right) \frac{\partial p}{\partial t}, \\ \frac{\partial^2 p}{\partial x^2} &= 2\Theta_0\Theta_p \frac{\partial^2 u}{\partial t^2} + (\Theta_u\Theta_p + \Theta_0^2) \frac{\partial^2 p}{\partial t^2} \\ &\quad + \left(\Theta_p \frac{\partial\Theta_0}{\partial t} + \Theta_0 \frac{\partial\Theta_p}{\partial t} + \frac{\partial\Theta_p}{\partial x} \right) \frac{\partial u}{\partial t} + \left(\Theta_p \frac{\partial\Theta_u}{\partial t} + \Theta_0 \frac{\partial\Theta_0}{\partial t} + \frac{\partial\Theta_0}{\partial x} \right) \frac{\partial p}{\partial t}. \end{aligned} \quad (3.52)$$

Multiplying Eqs. (3.51) and (3.52) by $2u$ and u^2 respectively, then summing using

$$\frac{\mathcal{D}^2}{\mathcal{D}t^2} = \frac{\partial^2}{\partial t^2} + 2u \frac{\partial^2}{\partial t \partial x} + u^2 \frac{\partial^2}{\partial x^2} + \frac{\mathcal{D}u}{\mathcal{D}t} \frac{\partial}{\partial x}$$

and setting $x = 0$ and $t \rightarrow 0^+$, we obtain the 2×2 linear system (3.50), to complete the proof. \square

Once the limiting values $(u_{tt})_*$ and $(p_{tt})_*$ are obtained by solving the system (3.50), the evaluation of $(u_{tx})_*$, $(p_{tx})_*$, $(u_{xx})_*$, and $(p_{xx})_*$ follows from Eqs. (3.51) and (3.52), and $(\rho_{tt})_*$ can then be obtained as follows.

Theorem 3.2. *The limiting value $(\rho_{tt})_*$ is given by*

$$(\rho_{tt})_* = \begin{cases} \frac{1}{h_* c_{s,*}^2} \left\{ \frac{\partial^2 p}{\partial t^2} - \frac{\partial(hc_s^2)}{\partial t} \frac{\partial \rho}{\partial t} - \frac{\partial^2 p}{\partial S \partial \rho} \frac{\partial \rho}{\partial t} \frac{\partial S}{\partial t} \right. \\ \left. - u^2 \frac{\partial^2 p}{\partial S^2} \left(\frac{\partial S}{\partial x} \right)^2 + \frac{\partial p}{\partial S} \left[\left(\frac{\partial u}{\partial t} - u \frac{\partial u}{\partial x} \right) \frac{\partial S}{\partial x} - u^2 \frac{\partial^2 S}{\partial x^2} \right] \right\}_*, & u_* > 0, \\ \frac{1}{(1 - s_* u_*^{-1})^2} \left(((1 - s u^{-1})^2 - 1) \mathcal{M}_1 - s^2 u^{-1} \mathcal{M}_2 - \frac{\mathcal{D}_s s}{\mathcal{D}t} \frac{\partial \rho}{\partial x} + \frac{\mathcal{D}_s^2 \rho}{\mathcal{D}t^2} \right)_*, & u_* < 0, \end{cases} \quad (3.53)$$

where S and s denote the entropy and the shock speed respectively, and

$$\left(\frac{\partial^2 S}{\partial x^2} \right)_* = \frac{1}{(\lambda_- - u)_*^2} \left\{ \left(\frac{\partial t}{\partial \alpha} \right)^{-2} \left(\frac{\partial^2 S}{\partial \alpha^2} \Big|_{\beta=\beta_l} - (\lambda_- - u) \frac{\partial^2 t}{\partial \alpha^2} \frac{\partial S}{\partial x} \right) + \mathcal{M}_s \frac{\partial S}{\partial x} \right\}_*, \quad (3.54)$$

$$\left(\frac{\mathcal{D}_s^2 \rho}{\mathcal{D}t^2} \right)_* = \left[\frac{C_{\rho 2}}{C_{\rho 1}} \frac{\mathcal{D}_s^2 p}{\mathcal{D}t^2} + \frac{\mathcal{D}_s}{\mathcal{D}t} \left(\frac{C_{\rho 2}}{C_{\rho 1}} \right) \frac{\mathcal{D}_s p}{\mathcal{D}t} + \frac{\mathcal{D}_s}{\mathcal{D}t} \left(\frac{C_{\rho 3}}{C_{\rho 1}} \frac{\mathcal{D}_s \bar{\rho}}{\mathcal{D}t} + \frac{C_{\rho 4}}{C_{\rho 1}} \frac{\mathcal{D}_s \bar{p}}{\mathcal{D}t} \right) \right]_*, \quad (3.55)$$

with

$$\begin{aligned} \mathcal{M}_s &:= \frac{\partial(u - \lambda_-)}{\partial t} + \lambda_- \frac{\partial(u - \lambda_-)}{\partial x} - (u - \lambda_-) \frac{\partial u}{\partial x}, \\ \mathcal{M}_1 &:= \frac{\partial(hc_s^2)^{-1}}{\partial t} \frac{\mathcal{D}p}{\mathcal{D}t} + \frac{1}{hc_s^2} \frac{\partial}{\partial t} \frac{\mathcal{D}p}{\mathcal{D}t} - \frac{\partial u}{\partial t} \frac{\partial \rho}{\partial x}, \\ \mathcal{M}_2 &:= \frac{\partial(hc_s^2)^{-1}}{\partial x} \frac{\mathcal{D}p}{\mathcal{D}t} + \frac{1}{hc_s^2} \frac{\partial}{\partial x} \frac{\mathcal{D}p}{\mathcal{D}t} - \frac{\partial u}{\partial x} \frac{\partial \rho}{\partial x} \end{aligned}$$

and $(\partial^2 t / \partial \alpha^2)_*$ given in Lemma 3.2.

Proof. (1). Let us first assume that $u_* > 0$ — i.e. the contact discontinuity is located at the right-hand side of the t -axis (cf. Figs. 1–2). Since $\mathcal{D}S/\mathcal{D}t = 0$, we have

$$\frac{\partial S}{\partial \alpha} = \frac{\partial t}{\partial \alpha} \left(\frac{\partial S}{\partial t} + \lambda_- \frac{\partial S}{\partial x} \right) = (\lambda_- - u) \frac{\partial t}{\partial \alpha} \frac{\partial S}{\partial x}.$$

Then on taking the partial derivative with respect to α and making use of (3.26), we have

$$\left. \frac{\partial^2 S}{\partial \alpha^2} \right|_{\beta=\beta_L} = \frac{\partial^2 S}{\partial \alpha^2} = (\lambda_- - u) \frac{\partial^2 t}{\partial \alpha^2} \frac{\partial S}{\partial x} + (\lambda_- - u)^2 \left(\frac{\partial t}{\partial \alpha} \right)^2 \frac{\partial^2 S}{\partial x^2} + \left(\frac{\partial t}{\partial \alpha} \right)^2 \mathcal{M}_S \frac{\partial S}{\partial x},$$

leading to Eq. (3.54) on setting $x = 0$ and $t \rightarrow 0^+$. Applying the chain rule to $p = p(\rho, S)$, we have

$$\frac{\partial p}{\partial t} = \frac{\partial p}{\partial \rho} \frac{\partial \rho}{\partial t} + \frac{\partial p}{\partial S} \frac{\partial S}{\partial t} = hc_s^2 \frac{\partial \rho}{\partial t} - u \frac{\partial p}{\partial S} \frac{\partial S}{\partial x}$$

and

$$\begin{aligned} \frac{\partial^2 p}{\partial t^2} &= hc_s^2 \frac{\partial^2 \rho}{\partial t^2} + \frac{\partial (hc_s^2)}{\partial t} \frac{\partial \rho}{\partial t} + \frac{\partial p}{\partial S} \left(\left(u \frac{\partial u}{\partial x} - \frac{\partial u}{\partial t} \right) \frac{\partial S}{\partial x} + u^2 \frac{\partial^2 S}{\partial x^2} \right) \\ &\quad + \frac{\partial^2 p}{\partial S \partial \rho} \frac{\partial \rho}{\partial t} \frac{\partial S}{\partial t} + u^2 \frac{\partial^2 p}{\partial S^2} \left(\frac{\partial S}{\partial x} \right)^2. \end{aligned} \quad (3.56)$$

The first case in (3.53) is thus proven, on reforming (3.56) and setting $x = 0$ and $t \rightarrow 0^+$.

(2). Let us now consider the case that $u_* < 0$. When the differential operator $\mathcal{D}_s \mathcal{D}_t$ is applied to the first equation in (3.46), on taking $x = 0$ and $t \rightarrow 0^+$ we obtain Eq. (3.55). On the other hand, since $\mathcal{D}_s^2 \rho / \mathcal{D}_t^2$ may be expanded to

$$\frac{\mathcal{D}_s^2 \rho}{\mathcal{D}_t^2} = \frac{\partial^2 \rho}{\partial t^2} + 2s \frac{\partial^2 \rho}{\partial t \partial x} + s^2 \frac{\partial^2 \rho}{\partial x^2} + \frac{\mathcal{D}_s s}{\mathcal{D}_t} \frac{\partial \rho}{\partial x},$$

from the first equation of (2.5) and the first equation in (2.4) we obtain

$$\frac{\partial^2 \rho}{\partial t \partial x} = u^{-1} \left(\mathcal{M}_1 - \frac{\partial^2 \rho}{\partial t^2} \right), \quad \frac{\partial^2 \rho}{\partial x^2} = u^{-1} \left[\mathcal{M}_2 - u^{-1} \left(\mathcal{M}_1 - \frac{\partial^2 \rho}{\partial t^2} \right) \right].$$

Combining the above three equations and setting $x = 0$ and $t \rightarrow 0^+$ give the second case of (3.53), and thus completes the proof. \square

Remark 3.6. For the ideal gas, $\partial p / \partial S$, $\partial^2 p / \partial \rho \partial S$ and $\partial^2 p / \partial S^2$ in (3.53) can be written explicitly as

$$\frac{\partial p}{\partial S} = \rho^\Gamma, \quad \frac{\partial^2 p}{\partial S \partial \rho} = \rho^{\Gamma-1}, \quad \frac{\partial^2 p}{\partial S^2} = 0.$$

II. Sonic case

Let us now consider that the left rarefaction wave is transonic, so that the t -axis is within the rarefaction wave — cf. Fig. 3. In this case, the local characteristic coordinate $\beta \in [\beta_L, \beta_1]$ where $\beta_1 := \lambda_-(U_1)$ is still needed, but the results in Propositions 3.1 and 3.2 are no longer available. Moreover, the Jacobian matrix $A(\mathbf{V})$ in (2.5) is singular at the sonic point $u = c_s$, so that the limiting value $(\mathbf{V}_x)_*$ or $(\mathbf{V}_{tt})_*$ cannot be calculated in the same way as in the non-sonic case. To avoid this difficulty, alternative third-order accurate approximations of $\mathbf{V}(\cdot, t_n + \Delta t/2)$ and $\mathbf{V}(\cdot, t_n + \Delta t)$ are introduced to replace $\mathbf{V}^{n+1/2}$ or $\mathbf{V}^{n+1,-}$ in (3.4) to resolve the GRP (3.6) as follows.

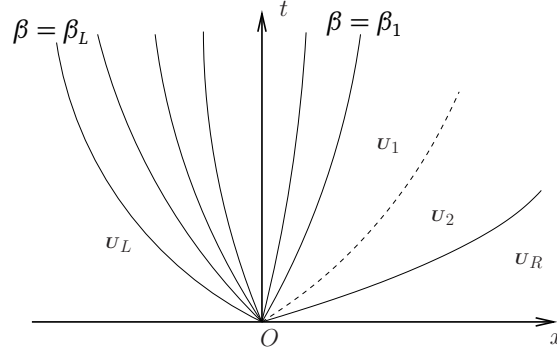


Figure 3: Schematic description of a local wave configuration for the GRP in the sonic case.

Theorem 3.3. *The directional derivatives of V along the characteristic curve $\lambda_- = \beta$ at the point $(0, \beta)$ are*

$$\mathcal{D}_- u(0, \beta) = \frac{\mathcal{D}_- \psi_-(0, \beta) - K(0, \beta) \mathcal{D}_- S(0, \beta)}{2\gamma^2(0, \beta)}, \quad (3.57)$$

$$\mathcal{D}_- p(0, \beta) = (\rho h \gamma^2 c_s)_{\alpha=0} \mathcal{D}_- u(0, \beta), \quad (3.58)$$

$$\mathcal{D}_- \rho(0, \beta) = \frac{\mathcal{D}_- p(0, \beta) - \frac{\partial p}{\partial S}(0, \beta) \mathcal{D}_- S(0, \beta)}{h(0, \beta) c_s^2(0, \beta)}, \quad (3.59)$$

with

$$\mathcal{D}_- \psi_-(0, \beta) = \left(\frac{\partial t}{\partial \alpha}(0, \beta) \right)^{-1} \frac{\partial \psi_-}{\partial \alpha}(0, \beta), \quad \mathcal{D}_- S(0, \beta) = \left(\frac{\partial t}{\partial \alpha}(0, \beta) \right)^{-1} \frac{\partial S}{\partial \alpha} \Big|_L, \quad (3.60)$$

where $\mathcal{D}_- v(0, \beta) := (\partial_t + \lambda_- \partial_x) v(0, \beta)$, $\frac{\partial \psi_-}{\partial \alpha}(0, \beta)$ is given by (3.25), and $\beta \in [\beta_L, \beta_1]$.

Proof. Using relation (2.9) and the first equation of (2.3) gives

$$\frac{\mathcal{D} \psi_-}{\mathcal{D} t} = \gamma^2 \frac{\mathcal{D} u}{\mathcal{D} t} + \frac{1}{\rho h c_s} \frac{\mathcal{D} p}{\mathcal{D} t}. \quad (3.61)$$

Combining this identity with the second and third equations of (2.4) we obtain

$$\begin{aligned} \mathcal{D}_- u &= \frac{\mathcal{D} u}{\mathcal{D} t} + (\lambda_- - u) \frac{\partial u}{\partial x} = \frac{\mathcal{D} u}{\mathcal{D} t} + \frac{c_s(1-u^2)}{1-uc_s} \gamma^2 \left(u \frac{\mathcal{D} u}{\mathcal{D} t} + \frac{1}{\rho h \gamma^2 c_s^2} \frac{\mathcal{D} p}{\mathcal{D} t} \right) \\ &= \frac{1-u^2}{1-uc_s} \left(\gamma^2 \frac{\mathcal{D} u}{\mathcal{D} t} + \frac{1}{\rho h c_s} \frac{\mathcal{D} p}{\mathcal{D} t} \right) = \frac{1-u^2}{1-uc_s} \frac{\mathcal{D} \psi_-}{\mathcal{D} t}, \end{aligned} \quad (3.62)$$

$$\begin{aligned} \mathcal{D}_- p &= \frac{\mathcal{D} p}{\mathcal{D} t} + (\lambda_- - u) \frac{\partial p}{\partial x} = \frac{\mathcal{D} p}{\mathcal{D} t} + \frac{c_s}{1-uc_s} \left(\rho h \gamma^2 \frac{\mathcal{D} u}{\mathcal{D} t} + u \frac{\mathcal{D} p}{\mathcal{D} t} \right) \\ &= \frac{\rho h c_s}{1-uc_s} \left(\gamma^2 \frac{\mathcal{D} u}{\mathcal{D} t} + \frac{1}{\rho h c_s} \frac{\mathcal{D} p}{\mathcal{D} t} \right) = \frac{\rho h c_s}{1-uc_s} \frac{\mathcal{D} \psi_-}{\mathcal{D} t} = \rho h \gamma^2 c_s \mathcal{D}_- u, \end{aligned} \quad (3.63)$$

where the second equation yields (3.58) on setting $\alpha = 0$. Then combining Eqs. (3.62) and (3.63) and using the relation (2.9), we obtain

$$\mathcal{D}_- \psi_- = \gamma^2 \mathcal{D}_- u + \frac{1}{\rho h c_s} \mathcal{D}_- p + K \mathcal{D}_- S = \frac{2}{1 - u c_s} \frac{\mathcal{D}_- \psi_-}{\mathcal{D}_- t} + K \mathcal{D}_- S,$$

or equivalently

$$\frac{\mathcal{D}_- \psi_-}{\mathcal{D}_- t} = \frac{1 - u c_s}{2} (\mathcal{D}_- \psi_- - K \mathcal{D}_- S), \quad (3.64)$$

and substituting this equation into (3.62) and setting $\alpha = 0$ gives (3.57). Applying the chain rule to $p = p(\rho, S)$, we obtain

$$\mathcal{D}_- p = \frac{\partial p}{\partial \rho} \mathcal{D}_- \rho + \frac{\partial p}{\partial S} \mathcal{D}_- S = h c_s^2 \mathcal{D}_- \rho + \frac{\partial p}{\partial S} \mathcal{D}_- S, \quad (3.65)$$

which can be reformed to give (3.59) on setting $\alpha = 0$. Consequently, the first equation in (3.10) yields

$$\frac{\partial \psi}{\partial \alpha} = \frac{\partial t}{\partial \alpha} \mathcal{D}_- \psi, \quad \frac{\partial S}{\partial \alpha} = \frac{\partial t}{\partial \alpha} \mathcal{D}_- S, \quad (3.66)$$

and we have (3.60) to complete the proof. \square

The following results may likewise be obtained.

Theorem 3.4. *The second-order directional derivatives of V along the characteristic curve $\lambda_- = \beta$ at the point $(0, \beta)$ can be calculated by*

$$\begin{aligned} \mathcal{D}_-^2 u(0, \beta) &= \mathcal{D}_- \left(\frac{1 - u^2}{1 - u c_s} \right) \left(\frac{1 - u c_s}{2} (\mathcal{D}_- \psi_- - K \mathcal{D}_- S) \right) (0, \beta) \\ &\quad + \frac{1 - u^2}{2} (\mathcal{D}_-^2 \psi_- - \mathcal{D}_- K \mathcal{D}_- S - K \mathcal{D}_-^2 S) (0, \beta) \\ &\quad + \frac{1 - u^2}{2(1 - u c_s)} \mathcal{D}_- (1 - u c_s) (\mathcal{D}_- \psi_- - K \mathcal{D}_- S) (0, \beta), \end{aligned} \quad (3.67)$$

$$\mathcal{D}_-^2 p(0, \beta) = \mathcal{D}_- (\rho h \gamma^2 c_s) (0, \beta) \mathcal{D}_- \psi_- (0, \beta) + (\rho h \gamma^2 c_s)_{\alpha=0} \mathcal{D}_-^2 u(0, \beta), \quad (3.68)$$

$$\mathcal{D}_-^2 \rho(0, \beta) = \frac{1}{h c_s^2} \left(\mathcal{D}_-^2 p - \mathcal{D}_- (h c_s^2) \mathcal{D}_- \rho - \mathcal{D}_- \left(\frac{\partial p}{\partial S} \right) \mathcal{D}_- S - \frac{\partial p}{\partial S} \mathcal{D}_-^2 S \right) (0, \beta), \quad (3.69)$$

with

$$\mathcal{D}_-^2 \psi_- (0, \beta) = \left(\frac{\partial t}{\partial \alpha} (0, \beta) \right)^{-2} \left(\frac{\partial^2 \psi_-}{\partial \alpha^2} (0, \beta) - \frac{\partial^2 t}{\partial \alpha^2} (0, \beta) \mathcal{D}_- \psi (0, \beta) \right), \quad (3.70)$$

$$\mathcal{D}_-^2 S (0, \beta) = \left(\frac{\partial t}{\partial \alpha} (0, \beta) \right)^{-2} \left(\frac{\partial^2 S}{\partial \alpha^2} \Big|_L - \frac{\partial^2 t}{\partial \alpha^2} (0, \beta) \mathcal{D}_- S (0, \beta) \right), \quad (3.71)$$

where $\mathcal{D}_-^2 \mathbf{v}(0, \beta) := (\partial_t + \lambda_- \partial_x)^2 \mathbf{v}(0, \beta)$, $\frac{\partial^2 t}{\partial \alpha^2}(0, \beta)$ and $\frac{\partial^2 \psi_-}{\partial \alpha^2}(0, \beta)$ are given by (3.28) and (3.35) respectively, and $\beta \in [\beta_L, \beta_1]$.

Proof. Taking the directional derivatives of (3.62) and (3.63) respectively along the characteristic curve λ_- gives

$$\mathcal{D}_-^2 u = \mathcal{D}_- \left(\frac{1-u^2}{1-uc_s} \right) \frac{\mathcal{D}_- \psi_-}{\mathcal{D}_- t} + \frac{1-u^2}{1-uc_s} \mathcal{D}_- \left(\frac{\mathcal{D}_- \psi_-}{\mathcal{D}_- t} \right), \quad (3.72)$$

$$\mathcal{D}_- p = \mathcal{D}_- (\rho h \gamma^2 c_s) \mathcal{D}_- u + \rho h \gamma^2 c_s \mathcal{D}_-^2 u, \quad (3.73)$$

where the second equation leads to (3.68) on setting $\alpha = 0$. Applying the differential operator \mathcal{D}_- to Eq. (3.64) gives

$$\mathcal{D}_- \left(\frac{\mathcal{D}_- \psi_-}{\mathcal{D}_- t} \right) = \frac{1-uc_s}{2} (\mathcal{D}_-^2 \psi_- - \mathcal{D}_- K \mathcal{D}_- S - K \mathcal{D}_-^2 S) + \frac{\mathcal{D}_- (1-uc_s)}{2} (\mathcal{D}_- \psi_- - K \mathcal{D}_- S),$$

and substituting this equation and Eq. (3.64) into Eq. (3.72) and setting $\alpha = 0$ yields (3.67). Similarly, from Eq. (3.65) we have

$$\mathcal{D}_-^2 p = \mathcal{D}_- (hc_s^2) \mathcal{D}_- \rho + hc_s^2 \mathcal{D}_-^2 \rho + \mathcal{D}_- \left(\frac{\partial p}{\partial S} \right) \mathcal{D}_- S + \frac{\partial p}{\partial S} \mathcal{D}_-^2 S,$$

which can be reformed to give Eq. (3.69) on setting $\alpha = 0$. Taking the partial derivatives of the two identities in (3.66) with respect to α and using the first relation of (3.10) gives

$$\begin{aligned} \frac{\partial^2 \psi}{\partial \alpha^2} &= \frac{\partial^2 t}{\partial \alpha^2} \mathcal{D}_- \psi + \left(\frac{\partial t}{\partial \alpha} \right)^2 \mathcal{D}_-^2 \psi, \\ \frac{\partial^2 S}{\partial \alpha^2} \Big|_L &= \frac{\partial^2 S}{\partial \alpha^2} = \frac{\partial^2 t}{\partial \alpha^2} \mathcal{D}_- S + \left(\frac{\partial t}{\partial \alpha} \right)^2 \mathcal{D}_-^2 S, \end{aligned}$$

whence Eqs. (3.70) and (3.71) respectively on rearranging and setting $\alpha = 0$, to complete the proof. \square

At the point $(x_\beta(\tau), \tau)$ on the characteristic curve $\lambda_- = \beta$, $\beta \in [\beta_L, \beta_1]$ and $\tau = \Delta t/2$, the value of V can be approximated to third-order accuracy by

$$V(x_\beta(\tau), \tau) \approx V(0, \beta) + \mathcal{D}_- V(0, \beta) \tau + \mathcal{D}_-^2 V(0, \beta) \frac{\tau^2}{2} =: \widehat{V}(\beta, \tau).$$

On the other hand, integrating $dx_\beta(t)/dt = \lambda_-(x_\beta(t), t)$ with respect to t yields

$$\begin{aligned} x_\beta(\tau) &= \int_0^\tau \lambda_-(x_\beta(t), t) dt = \int_0^\tau (\lambda_-(0, \beta) + \mathcal{D}_- \lambda_-(0, \beta) t) dt + \mathcal{O}(\tau^3) \\ &\approx \lambda_-(0, \beta) \tau + \mathcal{D}_- \lambda_-(0, \beta) \frac{\tau^2}{2} =: \widehat{x}(\beta, \tau). \end{aligned}$$

Consequently, for $\tau = \Delta t/2$ and Δt , employing respectively the Lagrange interpolation to the three-point set $\{\widehat{x}(\beta, \tau), \widehat{V}(\beta, \tau), \beta = \beta_L, 0, \beta_1\}$ gives corresponding quadratic polynomials approximating $V(x, \tau)$ — providing third-order accurate approximations for the values $V(x, \tau)$ at $x = 0$, as alternatives of $V^{n+1/2}$ and $V^{n+1,-}$ in (3.4).

III. Acoustic case

Let us now consider the acoustic case of the GRP (3.6) — i.e. $U_L = U_R$, and $U'_L \neq U'_R$ or $U''_L \neq U''_R$. It is simpler than the general case previously discussed, because $U_L = U_* = U_R$ and only linear waves emanate from the origin $(x, t) = (0, 0)$. For simplicity, we omit the subscripts $L, R, *$ to the variables U or V etc., because $U_L = U_* = U_R$. Without loss of generality, assume we have the limiting value $(V_t)_*$, and $\lambda_-(U) < 0$ and $\lambda_+(U) > 0$ corresponding to the local wave configuration — cf. Fig. 4.

Since the solution $U(x, t)$ is continuous across the characteristic curves λ_{\pm} , the k -order total derivatives along the trajectory $x'(t) = \lambda_{\pm}$ of the variable u or p satisfy

$$\begin{cases} ((\partial_t + \lambda_- \partial_x)^k u)_* = H^{(k),-}(u), & ((\partial_t + \lambda_+ \partial_x)^k u)_* = H^{(k),+}(u), \\ ((\partial_t + \lambda_- \partial_x)^k p)_* = H^{(k),-}(p), & ((\partial_t + \lambda_+ \partial_x)^k p)_* = H^{(k),+}(p), \end{cases} \quad (3.74)$$

where, $k = 1, 2$, and

$$H^{(k),+}(\varpi) := ((\partial_t + \lambda_+ \partial_x)^k \varpi)_R, \quad H^{(k),-}(\varpi) := ((\partial_t + \lambda_- \partial_x)^k \varpi)_L,$$

in which $\varpi = u$ or p . The time derivatives in $H^{(k),\pm}(\varpi)$ may be replaced with corresponding spatial derivatives by using (2.5) in the left and right smooth regions shown in Fig. 4, so that $H^{(k),-}(\varpi)$ (resp., $H^{(k),+}(\varpi)$) for $k = 1, 2$ may be calculated directly according to the initial data U_L, U'_L, U''_L (resp., U_R, U'_R, U''_R).

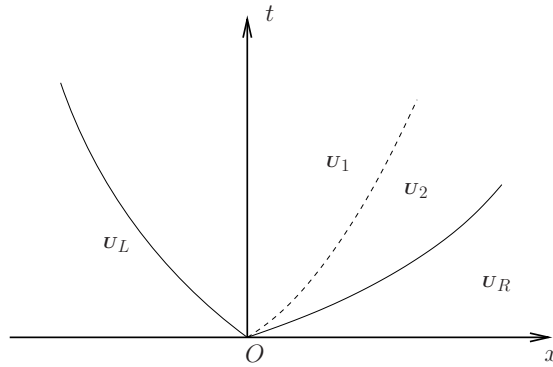


Figure 4: Schematic description of a local wave configuration for the GRP (3.6) in the acoustic case.

From (3.74) with $k = 1$, we have the limiting values $(u_x)_*$ and $(p_x)_*$ as follows:

$$\begin{aligned} (u_x)_* &= (H^{(1),+}(u) - H^{(1),-}(u)) / (\lambda_+ - \lambda_-), \\ (p_x)_* &= (H^{(1),+}(p) - H^{(1),-}(p)) / (\lambda_+ - \lambda_-). \end{aligned}$$

On the other hand, differentiating $p = p(\rho, S)$ with respect to x , using (2.6), and then setting $x = 0$ and $t \rightarrow 0^+$ leads to

$$\left(\frac{\partial \rho}{\partial x} \right)_* = \frac{1}{hc^2} \left(\frac{\partial p}{\partial x} - \frac{\partial p}{\partial S} \frac{\partial S}{\partial x} \right)_*. \quad (3.75)$$

Because $\mathcal{D}S/\mathcal{D}t = 0$ and the entropy S is continuous across the λ_{\pm} characteristic curve, we have

$$(S_x)_* = \frac{1}{\lambda_{\pm} - u} (S_t + \lambda_{\pm} S_x)_* = \begin{cases} \frac{1}{\lambda_- - u} (S_t + \lambda_- S_x)_L = (S_x)_L, & u_* > 0, \\ \frac{1}{\lambda_+ - u} (S_t + \lambda_+ S_x)_R = (S_x)_R, & u_* < 0. \end{cases} \quad (3.76)$$

Substituting into (3.75) then gives

$$(\rho_x)_* = \begin{cases} \frac{1}{hc_s^2} ((p_x)_* - p_S(S_x)_L), & u_* > 0, \\ \frac{1}{hc_s^2} ((p_x)_* - p_S(S_x)_R), & u_* < 0. \end{cases}$$

Using the known values \mathbf{V}_* , $(\mathbf{V}_t)_*$, and $(\mathbf{V}_x)_*$ gives the limiting values $(\mathbf{V}_{tt})_*$ as follows.

Theorem 3.5. *If $\lambda_- < 0$ and $\lambda_+ > 0$, then $(u_{tt})_*$ and $(p_{tt})_*$ can be obtained by solving a 6×6 linear algebraic system:*

$$\begin{pmatrix} 1 & \lambda_-^2 & 0 & 0 & 2\lambda_- & 0 \\ 1 & \lambda_+^2 & 0 & 0 & 2\lambda_+ & 0 \\ 0 & 0 & 1 & \lambda_-^2 & 0 & 2\lambda_- \\ 0 & 0 & 1 & \lambda_+^2 & 0 & 2\lambda_+ \\ 0 & \frac{\lambda_+ + \lambda_-}{2} & 0 & \frac{\lambda_+ - \lambda_-}{2} \Phi & 1 & 0 \\ 0 & \frac{\lambda_+ - \lambda_-}{2\Phi} & 0 & \frac{\lambda_+ + \lambda_-}{2} & 0 & 1 \end{pmatrix} \begin{pmatrix} (u_{tt})_* \\ (u_{xx})_* \\ (p_{tt})_* \\ (p_{xx})_* \\ (u_{tx})_* \\ (p_{tx})_* \end{pmatrix} = \mathbf{B}_{\text{rhs}}, \quad (3.77)$$

where the six-dimensional vector \mathbf{B}_{rhs} depends on the initial data \mathbf{U}_L , \mathbf{U}'_L , \mathbf{U}''_L , \mathbf{U}_R , \mathbf{U}'_R , \mathbf{U}''_R and the known limiting values \mathbf{V}_* , $(\mathbf{V}_t)_*$, $(\mathbf{V}_x)_*$. The limiting value $(\rho_{tt})_*$ is calculated as

$$(\rho_{tt})_* = \frac{1}{hc_s^2} \left\{ \frac{\partial p}{\partial S} \left[((u_t)_* - u(u_x)_*)(S_x)_Z - u^2 \left((S_{xx})_Z + \frac{1}{\lambda_Y - u} (S_x)_Z ((u_x)_* - (u_x)_Z) \right) \right] \right. \\ \left. + (p_{tt})_* - ((hc_s^2)_t \rho_t)_* - \frac{\partial^2 p}{\partial S \partial \rho} (\rho_t)_* (S_t)_* - u^2 \frac{\partial^2 p}{\partial S^2} (S_x)_Z^2 \right\}_*, \quad (3.78)$$

where the subscript Z and Y are respectively taken as L and $-$ if $u_* > 0$, R and $+$ otherwise.

Proof. (1). Using (3.74) with $k = 2$ and the relation

$$(\partial_t + \lambda_{\pm} \partial_x)^2 = \partial_t^2 + \lambda_{\pm}^2 \partial_x^2 + 2\lambda_{\pm} \partial_t \partial_x + \left(\frac{\partial \lambda_{\pm}}{\partial t} + \lambda_{\pm} \frac{\partial \lambda_{\pm}}{\partial x} \right) \partial_x$$

gives

$$\begin{aligned} ((\partial_t^2 + \lambda_{\mp}^2 \partial_x^2)u)_* + 2\lambda_{\mp} (u_{tx})_* &= H^{(2),\mp}(u) - (\partial_t \lambda_{\mp} + \lambda_{\mp} \partial_x \lambda_{\mp})_* (u_x)_*, \\ ((\partial_t^2 + \lambda_{\mp}^2 \partial_x^2)p)_* + 2\lambda_{\mp} (p_{tx})_* &= H^{(2),\mp}(p) - (\partial_t \lambda_{\mp} + \lambda_{\mp} \partial_x \lambda_{\mp})_* (p_x)_*. \end{aligned} \quad (3.79)$$

Utilizing the second and third equations in (2.5) gives

$$\begin{cases} \frac{\partial^2 u}{\partial t \partial x} + \frac{\lambda_+ + \lambda_-}{2} \frac{\partial^2 u}{\partial x^2} + \frac{\lambda_+ - \lambda_-}{2} \Phi \frac{\partial^2 p}{\partial x^2} = -\frac{1}{2} \frac{\partial(\lambda_+ + \lambda_-)}{\partial x} \frac{\partial u}{\partial x} - \frac{\partial}{\partial x} \left(\frac{\lambda_+ - \lambda_-}{2} \Phi \right) \frac{\partial p}{\partial x}, \\ \frac{\partial^2 p}{\partial t \partial x} + \frac{\lambda_+ + \lambda_-}{2} \frac{\partial^2 p}{\partial x^2} + \frac{\lambda_+ - \lambda_-}{2\Phi} \frac{\partial^2 u}{\partial x^2} = -\frac{1}{2} \frac{\partial(\lambda_+ + \lambda_-)}{\partial x} \frac{\partial p}{\partial x} - \frac{\partial}{\partial x} \left(\frac{\lambda_+ - \lambda_-}{2\Phi} \right) \frac{\partial u}{\partial x}. \end{cases}$$

Combining the above equations at $x = 0, t \rightarrow 0^+$ with (3.79) yields the 6×6 linear system (3.77).

(2). Applying the chain rule to $p = p(\rho, S)$, using (3.56) and setting $x = 0$ and $t \rightarrow 0^+$ gives

$$\begin{aligned} \left(\frac{\partial^2 \rho}{\partial t^2} \right)_* &= \frac{1}{hc_{s,*}^2} \left\{ \frac{\partial^2 p}{\partial t^2} - \frac{\partial(hc_s^2)}{\partial t} \frac{\partial \rho}{\partial t} - \frac{\partial^2 p}{\partial S \partial \rho} \frac{\partial \rho}{\partial t} \frac{\partial S}{\partial t} - u^2 \frac{\partial^2 p}{\partial S^2} \left(\frac{\partial S}{\partial x} \right)^2 \right. \\ &\quad \left. + \frac{\partial p}{\partial S} \left[\left(\frac{\partial u}{\partial t} - u \frac{\partial u}{\partial x} \right) \frac{\partial S}{\partial x} - u^2 \frac{\partial^2 S}{\partial x^2} \right] \right\}_*, \end{aligned} \quad (3.80)$$

and $(\partial^2 S / \partial x^2)_*$ may be calculated as follows. Assume that $u_* > 0$. Since the entropy S is continuous across the characteristic curve λ_- , we have

$$((\partial_t + \lambda_- \partial_x)^2 S)_* = ((\partial_t + \lambda_- \partial_x)^2 S)_L.$$

Inserting the relation

$$\begin{aligned} (\partial_t + \lambda_- \partial_x)^2 S &= (\partial_t + \lambda_- \partial_x) \left((\lambda_- - u) \frac{\partial S}{\partial x} \right) \\ &= ((\partial_t + \lambda_- \partial_x)(\lambda_- - u)) \frac{\partial S}{\partial x} + (\lambda_- - u) (\partial_t + \lambda_- \partial_x) \frac{\partial S}{\partial x} \\ &= (\lambda_- - u)^2 \frac{\partial^2 S}{\partial x^2} + (u - \lambda_-) \frac{\partial u}{\partial x} \frac{\partial S}{\partial x} + ((\partial_t + \lambda_- \partial_x)(\lambda_- - u)) \frac{\partial S}{\partial x} \end{aligned}$$

into the previous identity, and using (3.76) and the continuity of c_s across the characteristic curve λ_- , therefore gives

$$(S_{xx})_* = (S_{xx})_L + (\lambda_- - u)^{-1} (S_x)_L ((u_x)_* - (u_x)_L).$$

Similarly, for the case of $u_* < 0$ one has

$$(S_{xx})_* = (S_{xx})_R + (\lambda_+ - u)^{-1} (S_x)_L ((u_x)_* - (u_x)_R).$$

Then substituting into (3.80) and using (3.76) gives (3.78), so the proof is complete. \square

Table 1: Example 4.1: l^p errors in the density and convergence rates at $t = 0.5$ for GRP3, where $p = 1, 2, \infty$.

N	l^∞ -error	l^∞ -order	l^1 -error	l^1 -order	l^2 -error	l^2 -order
10	1.6917e-03	–	8.9413e-04	–	1.0517e-03	–
20	7.0977e-05	4.5750	3.5562e-05	4.6521	4.1823e-05	4.6523
40	3.2126e-06	4.4655	1.8519e-06	4.2632	2.0813e-06	4.3287
80	2.5675e-07	3.6453	1.5598e-07	3.5696	1.7319e-07	3.5871
160	2.7270e-08	3.2350	1.7154e-08	3.1847	1.9052e-08	3.1844
320	3.2629e-09	3.0631	2.0734e-09	3.0485	2.3029e-09	3.0484
640	4.5562e-10	2.8402	2.5738e-10	3.0100	2.8634e-10	3.0077
1280	5.3119e-11	3.1005	3.3817e-11	2.9281	3.7561e-11	2.9304
2560	6.3823e-12	3.0571	4.0583e-12	3.0588	4.5077e-12	3.0588

4. Numerical Experiments

We have solved several cases of the 1D RHD equations (2.1), to verify the accuracy and the discontinuity-resolving capability of the proposed third-order accurate GRP scheme (henceforth abbreviated “GRP3”), in comparison with the second-order accurate GRP scheme (abbreviated by “GRP2”) [21]. Unless specifically stated, all computations were restricted to the equation of state (2.2) with the adiabatic index $\gamma = 5/3$, and the CFL number $C_{\text{cfl}} = 0.4$ for GRP3, while the parameters in GRP2 are the same as those in Ref. [21]. The numerical solutions obtained via GRP2 and GRP3 respectively are annotated by the symbols “*” and “o” below, while the exact or reference solutions are represented by the solid lines.

Example 4.1 (Accuracy test). This example is used to check the accuracy of the GRP3 for the smooth solution

$$V(x, t) = (1 + 0.2 \sin(2\pi(x - ut)), 0.2, 1)^T,$$

which describes a sine wave propagating periodically within the domain $\Omega = [0, 1]$. The computational domain Ω is divided into N uniform cells and periodic boundary conditions are specified. Table 1 gives the l^p errors in the density and corresponding convergence rates for GRP3, where $p = 1, 2, \infty$. The data show that the convergence rate can be almost of third-order.

Example 4.2 (Riemann problem I). The initial conditions of the first Riemann or (relativistic) shock tube problem are

$$V(x, 0) = \begin{cases} (10, 0, 40/3)^T, & x < 0.5, \\ (1, 0, 10^{-6})^T, & x > 0.5, \end{cases} \quad (4.1)$$

which will evolve as a left-moving rarefaction wave, a constant discontinuity, and a right-moving shock wave.

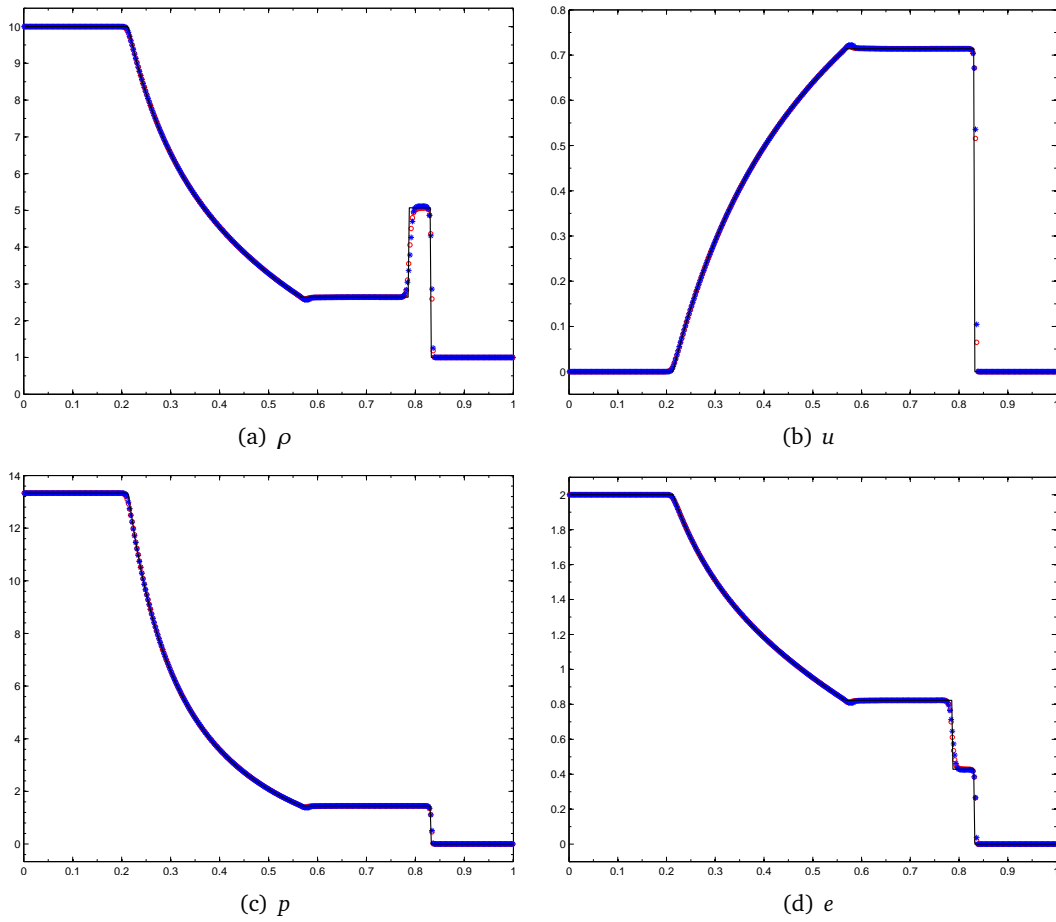


Figure 5: Example 4.2: density ρ , the velocity u , the pressure p and internal energy e at $t = 0.4$ with 400 uniform cells.

Fig. 5 displays numerical solutions at $t = 0.4$, obtained using GRP3 and GRP2 with 400 uniform cells, seen to be in good agreement with the exact solutions. Evidently, GRP2 and GRP3 can well resolve discontinuities.

Example 4.3 (Riemann problem II). This is a ultra-relativistic (i.e. $\gamma \gg 1$) shock tube problem similar to Example 4.2, but more extreme and difficult. The initial conditions are

$$\mathbf{v}(x, 0) = \begin{cases} (10, 0, 10^3)^T, & x < 0.5, \\ (1, 0, 10^{-2})^T, & x > 0.5. \end{cases} \quad (4.2)$$

Fig. 6 shows the numerical solutions at $t = 0.4$, obtained using GRP3 and GRP2 with 400 uniform cells, and again showing good agreement with the exact solutions. Due to the appearance of the ultra-relativistic regime, the initial discontinuity evolves a heavily curved profile for the rarefaction fan and two strong discontinuities. It is seen in Fig. 6(a)

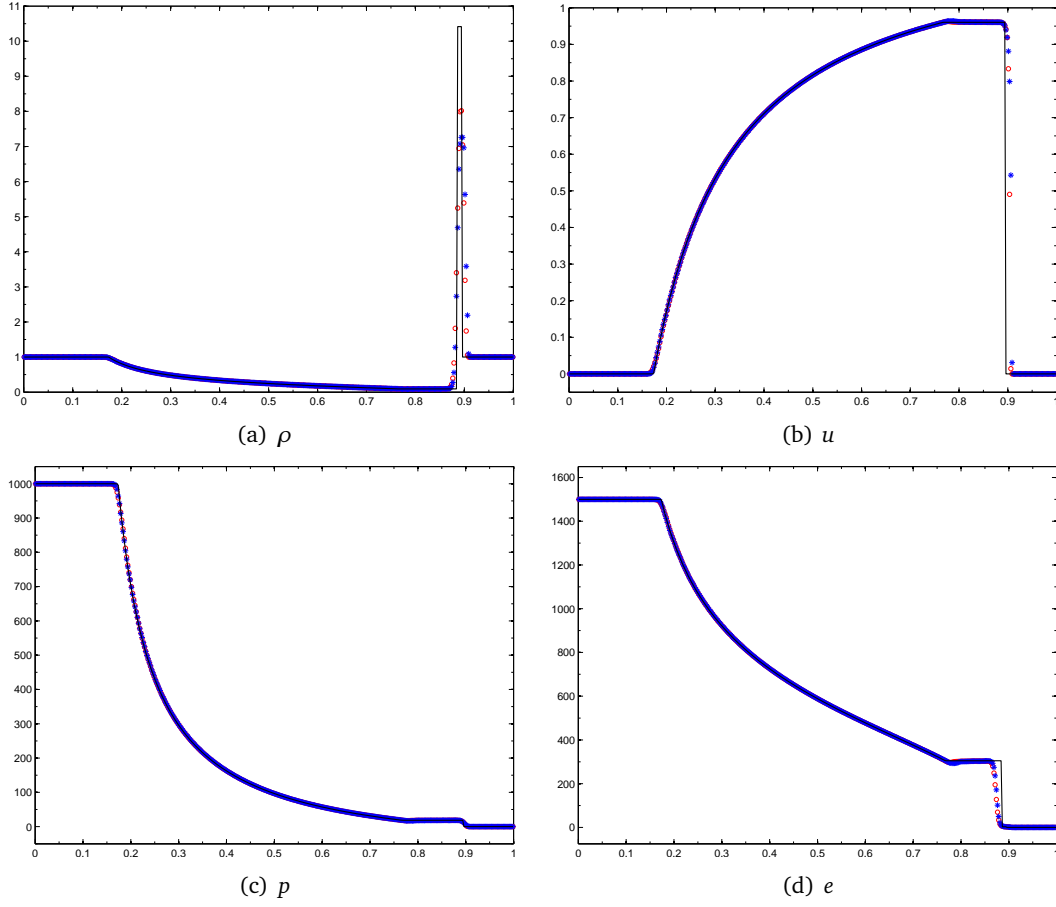


Figure 6: Example 4.3: density ρ , the velocity u , the pressure p and internal energy e at $t = 0.4$ with 400 uniform cells.

that GRP3 has a better resolution for the sharp solution ρ near the right-hand side of the contact discontinuity. The CFL number $C_{cfl} = 0.3$ for GRP3 in this computation.

We see that the main differences between the solution of relativistic shock tube problems and their non-relativistic counterparts are due to the nonlinear addition of velocities and the Lorentz contraction — the first feature yields a curved profile for the rarefaction fan, as opposed to a linear one in the non-relativistic case; the second latter narrows the shock plateau. These effects, especially the narrowed shock plateau, become particularly noticeable in the ultra-relativistic regime.

Example 4.4 (Riemann problem III). Another Riemann problem involved the initial data

$$V(x, 0) = \begin{cases} (1, -2, 0.4)^T, & x < 0.5, \\ (1, 2, 0.4)^T, & x > 0.5, \end{cases} \quad (4.3)$$

growing into both left- and right-moving rarefaction waves such that the low density region

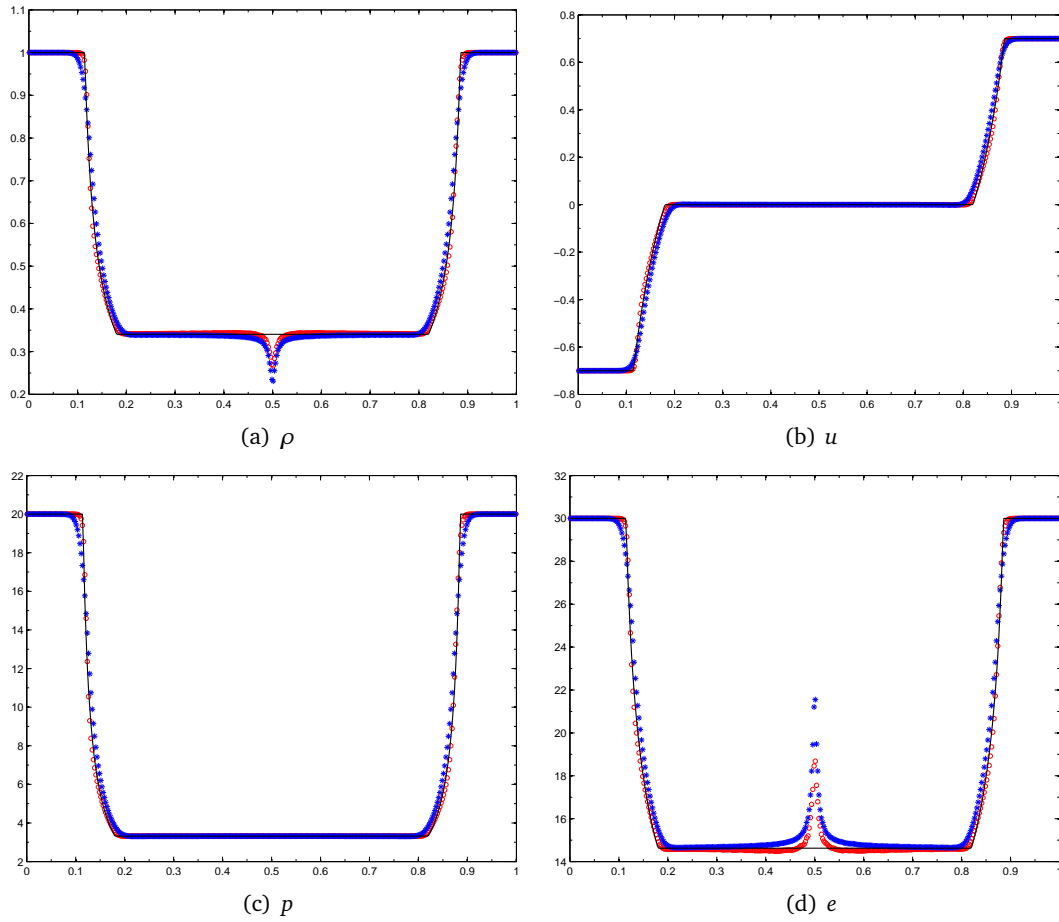


Figure 7: Example 4.4: density ρ , the velocity u , the pressure p and internal energy e at $t = 0.4$ with 400 uniform cells.

appears around $x = 0.5$. Fig. 7 presents the density, velocity, pressure and internal energy at $t = 0.4$ obtained using GRP3 and GRP2 with 400 uniform cells. We see that both GRP schemes can well preserve the positivity of the density and the pressure. Although there exists serious undershoots in the density at $x = 0.5$ for the two schemes, GRP3 produces a relatively good approximation. The CFL number $C_{\text{cfl}} = 0.3$ for GRP3 in this computation.

Example 4.5 (Density perturbation problem). This is a more general Cauchy problem obtained by including a density perturbation in the initial data of the corresponding Riemann problem [23] in order to test the ability of the shock-capturing schemes to resolve small-scale flow features, which may give a good indication of the numerical (artificial) viscosity of the scheme. The initial data taken were

$$v(x, 0) = \begin{cases} (5, 0, 50)^T, & x < 0.5, \\ (2 + 0.3 \sin(50x), 0, 5)^T, & x > 0.5. \end{cases} \quad (4.4)$$

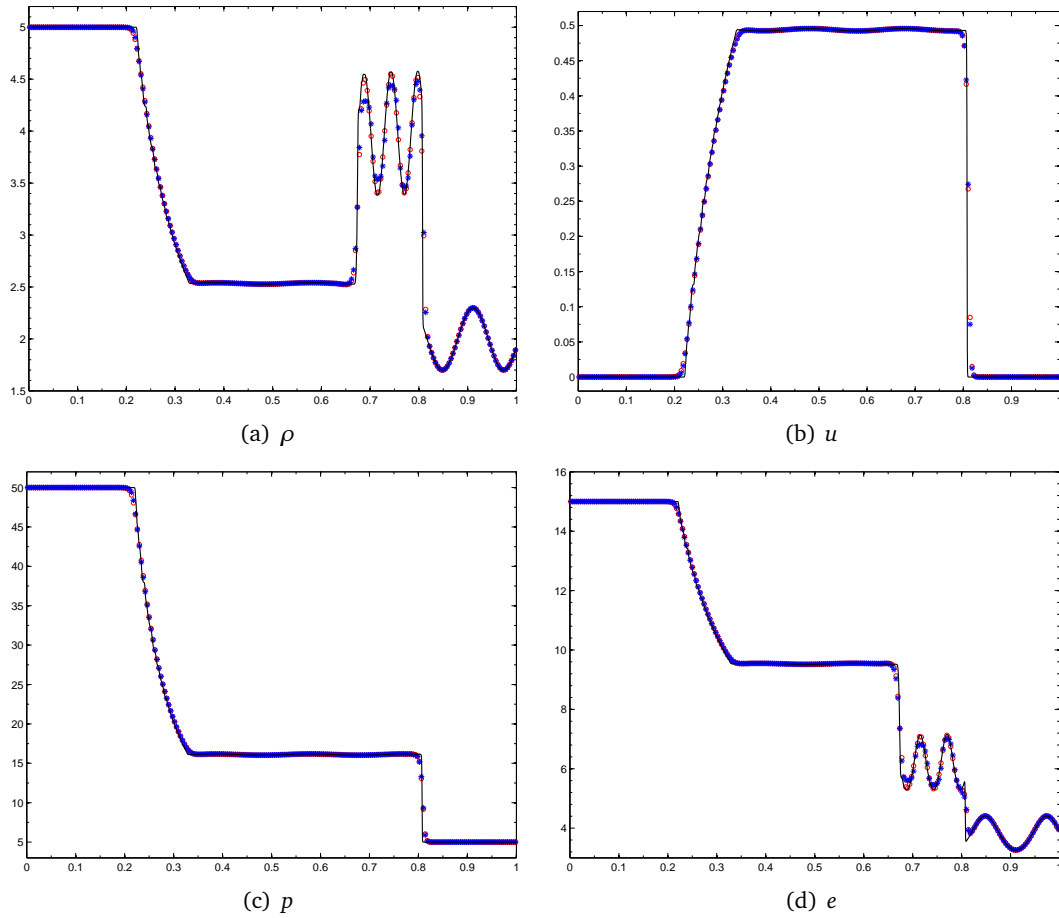


Figure 8: Example 4.5: density ρ (and its close-up), the velocity u , and the pressure p at $t = 0.35$ with 400 uniform cells.

Fig. 8 shows the numerical results at $t = 0.35$ obtained using GRP3 and GRP2 with 250 uniform cells, where the reference solutions (solid lines) obtained by GRP2 with 2000 uniform cells are also displayed for comparison. It can be seen that GRP3 resolves the high frequency waves much better than GRP2.

Example 4.6 (Collision of two relativistic blast waves). The last example simulated the collision of two strong relativistic blast waves [12]. The initial data for this initial-boundary-value problems were consisting of three constant states of an ideal gas with $\Gamma = 1.4$, at rest in the domain $[0, 1]$ with outflow boundary conditions at $x = 0$ and 1. The density is everywhere unity, and the pressure is 1000 for $0 < x < 0.1$, 100 for $0.9 < x < 1$, and 0.01 in the intervening interval. Two strong blast waves develop and collide, producing a new contact discontinuity. Fig. 9 gives a close-up of the numerical solutions obtained at $t = 0.43$ using GRP3 and GRP2 with 2000 uniform cells, where the solid lines denote the exact solutions. We see that both GRP schemes can well resolve the discontinuities, and clearly capture the relativistic wave configurations generated by the interaction of the two

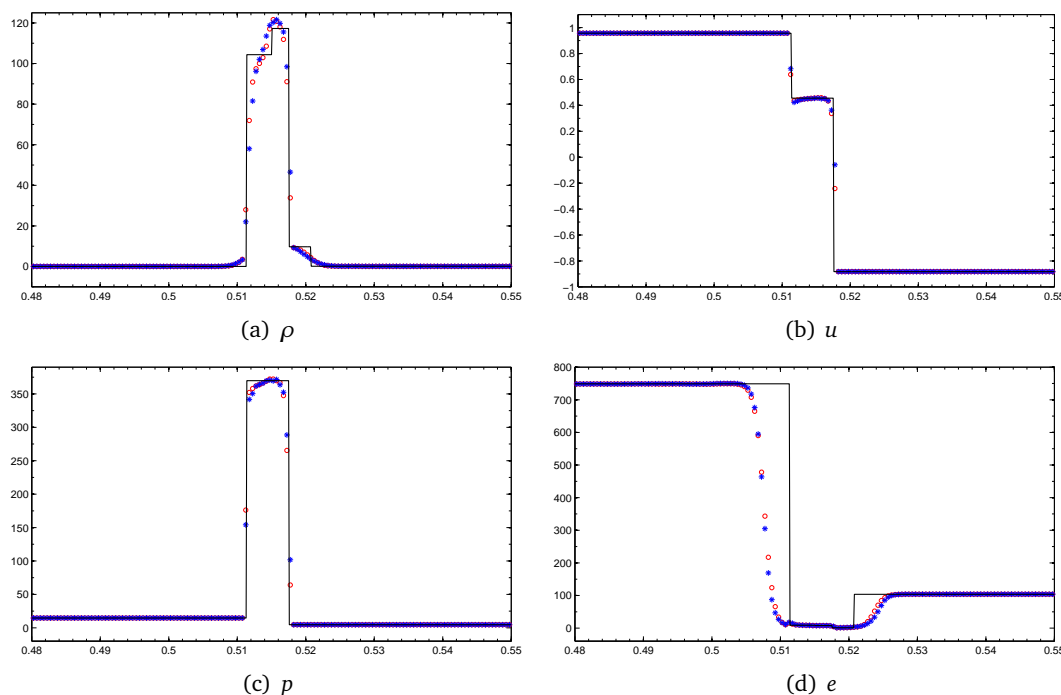


Figure 9: Example 4.6: close-up of the numerical solutions at $t = 0.43$ with 2000 uniform cells.

strong relativistic blast waves, with GRP3 exhibiting a little better resolution than GRP2. The CFL number $C_{\text{cfl}} = 0.3$ for GRP3 in this computation.

5. Conclusions

Relativistic hydrodynamics (RHD) plays a major role in many fields of modern physics such as astrophysics, high-energy or nuclear physics and its numerical simulation is indispensable. In this article, a third-order accurate direct Eulerian generalised Riemann problem (GRP) scheme is analytically derived for the 1D special RHD equations. The higher-order WENO initial reconstruction is employed, and the local GRPs in the Eulerian formulation are directly and analytically resolved to third-order accuracy via the Riemann invariants and Rankine-Hugoniot jump conditions, to get the approximate states for the fluxes. In comparison to the second-order accurate GRP scheme proposed in Ref. [21], in the non-sonic case the limiting values of the first-order and second-order time derivatives of the fluid variables at the singular point are derived for the calculation of the approximate states. Unfortunately, for the transonic case where a rarefaction wave appears in the local GRP, the Jacobian matrix in (2.5) is not always nonsingular within the transonic rarefaction wave, so that the first-order spatial derivatives and the second-order time derivatives of fluid variables cannot be calculated. For this reason, the approximate states in the numerical fluxes are obtained differently, based on the analytical resolution of the transonic rarefaction wave and quadratic polynomial interpolation within the transonic rarefaction

wave. Several numerical examples are provided to demonstrate the accuracy and effectiveness of the proposed GRP scheme, in comparison to the earlier second-order accurate GRP scheme [21]. Our results show that the proposed third-order accurate GRP scheme is more accurate, with higher resolution but with a more technical derivation than the second-order accurate GRP scheme.

Acknowledgements

This work was partially supported by the National Natural Science Foundation of China (Nos. 10925101 & 91330205).

Appendices

A. Derivation of $\frac{\partial^2 t}{\partial \alpha^2}(0, \beta_L)$ in (3.28)

Due to (3.15), one can derive the asymptotic expressions of $\partial x/\partial \alpha$ and $\partial t/\partial \alpha$ for substitution into the first equation of (3.10), to get

$$\begin{aligned} & \beta \beta_L^{-1} \exp \left(\int_{\beta_L}^{\beta} \frac{d\omega}{u(0, \omega) - \omega} \right) + 2\alpha \epsilon(\alpha, \beta) + \frac{\partial \epsilon}{\partial \alpha}(\alpha, \beta) \alpha^2 \\ & = \lambda_-(\alpha, \beta) \left(\beta_L^{-1} \exp \left(\int_{\beta_L}^{\beta} \frac{d\omega}{u(0, \omega) - \omega} \right) + 2\alpha \eta(\alpha, \beta) + \frac{\partial \eta}{\partial \alpha}(\alpha, \beta) \alpha^2 \right). \end{aligned}$$

Introducing Taylor expansions of $\lambda_-(\alpha, \beta)$, $\epsilon(\alpha, \beta)$ and $\eta(\alpha, \beta)$ about $\alpha = 0$ and neglecting the $\mathcal{O}(\alpha^2)$ terms, we have

$$2\epsilon(0, \beta) = 2\beta \eta(0, \beta) + \frac{\partial \lambda_-}{\partial \alpha}(0, \beta) \beta_L^{-1} \exp \left(\int_{\beta_L}^{\beta} \frac{d\omega}{u(0, \omega) - \omega} \right). \quad (\text{A.1})$$

On setting $\beta = \beta_L$, and considering $\epsilon(\alpha, \beta_L) = 0$ obtained by comparing the second equation at (α, β_L) in (3.15) to $x(\alpha, \beta_L) = x_{\text{ass}}(\alpha, \beta_L) = \alpha$, one has

$$\eta(0, \beta_L) = \beta_L^{-1} \epsilon(0, \beta_L) - \frac{1}{2} \beta_L^{-2} \frac{\partial \lambda_-}{\partial \alpha}(0, \beta_L) = -\frac{1}{2} \beta_L^{-2} \frac{\partial \lambda_-}{\partial \alpha}(0, \beta_L). \quad (\text{A.2})$$

Thus from the first equation of (3.15), it follows that

$$\frac{\partial^2 t}{\partial \alpha^2}(0, \beta_L) = 2\eta(0, \beta_L) = -\beta_L^{-2} \frac{\partial \lambda_-}{\partial \alpha}(0, \beta_L). \quad (\text{A.3})$$

B. Calculation of $\frac{\partial^2 \lambda_-}{\partial \alpha \partial \beta}(0, \beta)$ in (3.30)

For the ideal gas law (2.2), using (2.8) and (2.12) we have

$$\psi_{\pm} = \frac{1}{2} \ln \left(\frac{1+u}{1-u} \right) \mp (\Gamma - 1)^{-1/2} \ln \left(\frac{(\Gamma - 1)^{1/2} + c_s}{(\Gamma - 1)^{1/2} - c_s} \right), \quad (\text{B.1})$$

yielding

$$\psi_- + \psi_+ = \ln \left(\frac{1+u}{1-u} \right), \quad \psi_- - \psi_+ = 2(\Gamma - 1)^{-1/2} \ln \left(\frac{(\Gamma - 1)^{1/2} + c_s}{(\Gamma - 1)^{1/2} - c_s} \right) \quad (\text{B.2})$$

and

$$0 = \frac{\partial \psi_-}{\partial \beta}(0, \beta) = \frac{1}{1-u^2(0, \beta)} \frac{\partial u}{\partial \beta}(0, \beta) + \frac{2}{\Gamma - 1 - c_s^2(0, \beta)} \frac{\partial c_s}{\partial \beta}(0, \beta), \quad (\text{B.3})$$

on setting $\alpha = 0$ and taking partial derivative of ψ_- with respect to β . On the other hand, using

$$\beta = \lambda_-(0, \beta) = \frac{u(0, \beta) - c_s(0, \beta)}{1 - u(0, \beta)c_s(0, \beta)},$$

or equivalently,

$$u(0, \beta) = \frac{\beta + c_s(0, \beta)}{1 + \beta c_s(0, \beta)},$$

one has

$$\frac{\partial u}{\partial \beta}(0, \beta) = \frac{1 - c_s^2(0, \beta)}{(1 + \beta c_s(0, \beta))^2} + \frac{1 - \beta^2}{(1 + \beta c_s(0, \beta))^2} \frac{\partial c_s}{\partial \beta}(0, \beta). \quad (\text{B.4})$$

Combining (B.3) and (B.4) gives

$$\frac{\partial u}{\partial \beta}(0, \beta) = \frac{1 - c_s^2}{(1 + \beta c_s)^2 + \frac{(\Gamma - 1 - c_s^2)(1 - \beta^2)}{2(1 - u^2)}}, \quad \frac{\partial c_s}{\partial \beta}(0, \beta) = \frac{c_s^2 - 1}{1 - \beta^2 + \frac{2(1 + \beta c_s)^2(1 - u^2)}{\Gamma - 1 - c_s^2}}, \quad (\text{B.5})$$

where the values of u and c_s are taken at the point $(0, \beta)$.

Taking partial derivative of the first equation in (B.2) with respect to α then gives

$$\frac{\partial u}{\partial \alpha} = \frac{1}{2}(1 - u^2) \left(\frac{\partial \psi_+}{\partial \alpha} + \frac{\partial \psi_-}{\partial \alpha} \right),$$

which yields

$$\frac{\partial^2 u}{\partial \alpha \partial \beta}(0, \beta) = \left(\frac{1}{2}(1 - u^2) \left(\frac{\partial^2 \psi_+}{\partial \alpha \partial \beta} + \frac{\partial^2 \psi_-}{\partial \alpha \partial \beta} \right) - u \frac{\partial u}{\partial \beta} \left(\frac{\partial \psi_+}{\partial \alpha} + \frac{\partial \psi_-}{\partial \alpha} \right) \right) (0, \beta) \quad (\text{B.6})$$

on considering its partial derivative with respect to β and setting $\alpha = 0$. Similarly, considering the second equation in (B.2) we have

$$\frac{\partial^2 c_s}{\partial \alpha \partial \beta}(0, \beta) = \left(\frac{\Gamma - 1 - c_s^2}{4} \left(\frac{\partial^2 \psi_-}{\partial \alpha \partial \beta} - \frac{\partial^2 \psi_+}{\partial \alpha \partial \beta} \right) - \frac{2c_s}{\Gamma - 1 - c_s^2} \frac{\partial c_s}{\partial \alpha} \frac{\partial c_s}{\partial \beta} \right) (0, \beta). \quad (\text{B.7})$$

It is notable that the calculations of $\frac{\partial^2 \psi_{\pm}}{\partial \alpha \partial \beta}(0, \beta)$, $\frac{\partial \psi_{\pm}}{\partial \alpha}(0, \beta)$ and $\frac{\partial u}{\partial \beta}(0, \beta)$, $\frac{\partial c_s}{\partial \beta}(0, \beta)$ in (B.6)–(B.7) were given in Lemma 3.1 and Eqs. (B.5) respectively, so $\frac{\partial^2 u}{\partial \alpha \partial \beta}(0, \beta)$ and $\frac{\partial^2 c_s}{\partial \alpha \partial \beta}(0, \beta)$ can be calculated from (B.6) and (B.7), respectively. Based on these limiting values, the calculation of $\frac{\partial^2 \lambda_-}{\partial \alpha \partial \beta}(0, \beta)$ in (3.30) may be completed using

$$\begin{aligned} \frac{\partial^2 \lambda_-}{\partial \alpha \partial \beta} &= \frac{1}{(1 - uc_s)^2} \left((1 - c_s^2) \frac{\partial^2 u}{\partial \alpha \partial \beta} - (1 - u^2) \frac{\partial^2 c_s}{\partial \alpha \partial \beta} - 2c_s \frac{\partial u}{\partial \beta} \frac{\partial c_s}{\partial \alpha} + 2u \frac{\partial u}{\partial \alpha} \frac{\partial c_s}{\partial \beta} \right) \\ &\quad + \frac{2}{(1 - uc_s)^3} \left((1 - c_s^2) \frac{\partial u}{\partial \beta} - (1 - u^2) \frac{\partial c_s}{\partial \beta} \right) \left(c_s \frac{\partial u}{\partial \alpha} + u \frac{\partial c_s}{\partial \alpha} \right), \end{aligned}$$

derived by taking the mixed second partial derivative of the first equation in (2.2) with respect to α and β and using of the chain rule.

References

- [1] M. Ben-Artzi and J. Falcovitz, *A second-order Godunov-type scheme for compressible fluid dynamics*, J. Comput. Phys. **55**, 1–32 (1984).
- [2] M. Ben-Artzi and J. Falcovitz, *Generalized Riemann Problems in Computational Fluid Dynamics*, Cambridge University Press, 2003.
- [3] M. Ben-Artzi and J.Q. Li, *Hyperbolic balance laws: Riemann invariants and the generalized Riemann problem*, Numer. Math., **106**, 369–425 (2007).
- [4] M. Ben-Artzi, J.Q. Li, and G. Warnecke, *A direct Eulerian GRP scheme for compressible fluid flows*, J. Comput. Phys. **218**, 19–43 (2006).
- [5] J.A. Font, *Numerical hydrodynamics and magnetohydrodynamics in general relativity*, Living Rev. Relativity **11**, 7 (2008).
- [6] E. Han, J.Q. Li, and H.Z. Tang, *An adaptive GRP scheme for compressible fluid flows*, J. Comput. Phys. **229**, 1448–1466 (2010).
- [7] E. Han, J.Q. Li, and H.Z. Tang, *Accuracy of the adaptive GRP scheme and the simulation of 2-D Riemann problems for compressible Euler equations*, Commun. Comput. Phys. **10**, 577–606 (2011).
- [8] J.Q. Li and G.X. Chen, *The generalized Riemann problem method for the shallow water equations with bottom topography*, Int. J. Numer. Meth. in Eng. **65**, 834–862 (2006).
- [9] J.Q. Li, Q.B. Li, and K. Xu, *Comparison of the generalized Riemann solver and the gas-kinetic scheme for inviscid compressible flow simulations*, J. Comput. Phys. **230**, 5080–5099 (2011).
- [10] J. Luo and K. Xu, *A high-order multidimensional gas-kinetic scheme for hydrodynamic equations*, Sci. China Tech. Sci. **56**, 2370–2384 (2013).
- [11] J.M. Martí and E. Müller, *The analytical solution of the Riemann problem in relativistic hydrodynamics*, J. Fluid Mech. **258**, 317–333 (1994).

- [12] J.M. Martí and E. Müller, *Extension of the piecewise parabolic method to one dimensional relativistic hydrodynamics*, J. Comput. Phys. **123**, 1–14 (1996).
- [13] J.M. Martí and E. Müller, *Numerical hydrodynamics in special relativity*, Living Rev. Relativity **6**, 7 (2003).
- [14] J.Z. Qian, J.Q. Li, and S.H. Wang, *The generalized Riemann problems for compressible fluid flows: Towards high order*, J. Comput. Phys. **259**, 358–389 (2014).
- [15] H.Z. Tang and T. Tang, *Adaptive mesh methods for one- and two-dimensional hyperbolic conservation laws*, SIAM J. Numer. Anal. **41**, 487–515 (2003).
- [16] J.R. Wilson, *Numerical study of fluid flow in a Kerr space*, Astrophys. J. **173**, 431–438 (1972).
- [17] J.R. Wilson and G.J. Mathews, *Relativistic Numerical Hydrodynamics*, Cambridge University Press, 2003.
- [18] K.L. Wu and H.Z. Tang, *Finite volume local evolution galerkin method for two-dimensional relativistic hydrodynamics*, J. Comput. Phys. **256**, 277–307 (2014).
- [19] K.L. Wu, Z.C. Yang, and H.Z. Tang, *A third-order accurate direct Eulerian GRP scheme for the Euler equations in gas dynamics*, J. Comput. Phys. **264**, 177–208 (2014).
- [20] J.P. Xu, M. Luo, J.C. Hu, S.Z. Wang, B. Qi, and Z.G. Qiao, *A direct Eulerian GRP Scheme for the prediction of gas-liquid two-phase flow in HTHP transient wells*, Abs. Appl. Anal. **2013**, 171732(2013).
- [21] Z.C. Yang, P. He, and H.Z. Tang, *A direct Eulerian GRP scheme for relativistic hydrodynamics: One-dimensional case*, J. Comput. Phys. **230**, 7964–7987 (2011).
- [22] Z.C. Yang and H.Z. Tang, *A direct Eulerian GRP scheme for relativistic hydrodynamics: Two-dimensional case*, J. Comput. Phys. **231**, 2116–2139 (2012).
- [23] L.D. Zanna and N. Bucciantini, *An efficient shock-capturing central-type scheme for multidimensional relativistic flows, I: hydrodynamics*, Astron. Astrophys. **390**, 1177–1186 (2002).
- [24] J. Zhao and H.Z. Tang, *Runge-Kutta discontinuous Galerkin methods with WENO limiters for the special relativistic hydrodynamics*, J. Comput. Phys. **242**, 138–168 (2013).